HHS Public Access

Author manuscript

Brain Behav Immun. Author manuscript; available in PMC 2024 May 01.

Published in final edited form as:

Brain Behav Immun. 2023 May ; 110: 260–275. doi:10.1016/j.bbi.2023.03.002.

Reduction in GABAB on glia induce Alzheimer's disease related changes

Amanda M. Leisgang Osse[1,*], **Ravi S. Pandey**[2], **Ryan A. Wirt**[3], **Andrew A. Ortiz**[1], **Arnold Salazar**[1], **Michael Kimmich**[1], **Erin N. Strom**[1], **Adrian Oblak**[4], **Bruce Lamb**[4], **James M. Hyman**[3], **Gregory W. Carter**[2], **Jefferson Kinney**[1]

[1]University of Nevada, Las Vegas, Department of Brain Health, 4505 S. Maryland Parkway, Las Vegas, NV 89154

[2]The Jackson Laboratory, Genomic Medicine, 10 Discovery Drive, Farmington, CT 06032

[3]University of Nevada, Las Vegas, Department of Psychology, 4505 S. Maryland Parkway, Las Vegas, NV 89154

[4]Indiana University, School of Medicine, 340 W 10th Street, Indianapolis, IN 46202

Abstract

Alzheimer's Disease (AD) is a neurodegenerative disorder characterized by beta-amyloid plaques (Aβ), neurofibrillary tangles (NFT), and neuroinflammation. Data have demonstrated that neuroinflammation contributes to Aβ and NFT onset and progression, indicating inflammation and glial signaling is vital to understanding AD. A previous investigation demonstrated a significant decrease of the $GABA_B$ receptor ($GABA_BR$) in APP/PS1 mice (A. M. Salazar et al., 2021). To determine if changes in $GABA_BR$ restricted to glia serve a role in AD, we developed a mouse model with a reduction of $GABA_BR$ restricted to macrophages, GAB/CX3ert. This model exhibits alterations in gene expression and electrophysiological alterations similar to amyloid mouse models of AD. Crossing the GAB/CX3ert mouse with APP/PS1 resulted in significant increases in Aβ pathology. Our data demonstrates that decreased $GABA_BR$ on macrophages leads to several changes observed in AD mouse models, as well as exacerbation of AD pathology when crossed with existing models. These data suggest a novel mechanism in AD pathogenesis.

Graphical Abstract

[*]Corresponding author: amanda.leisgang@unlv.edu.

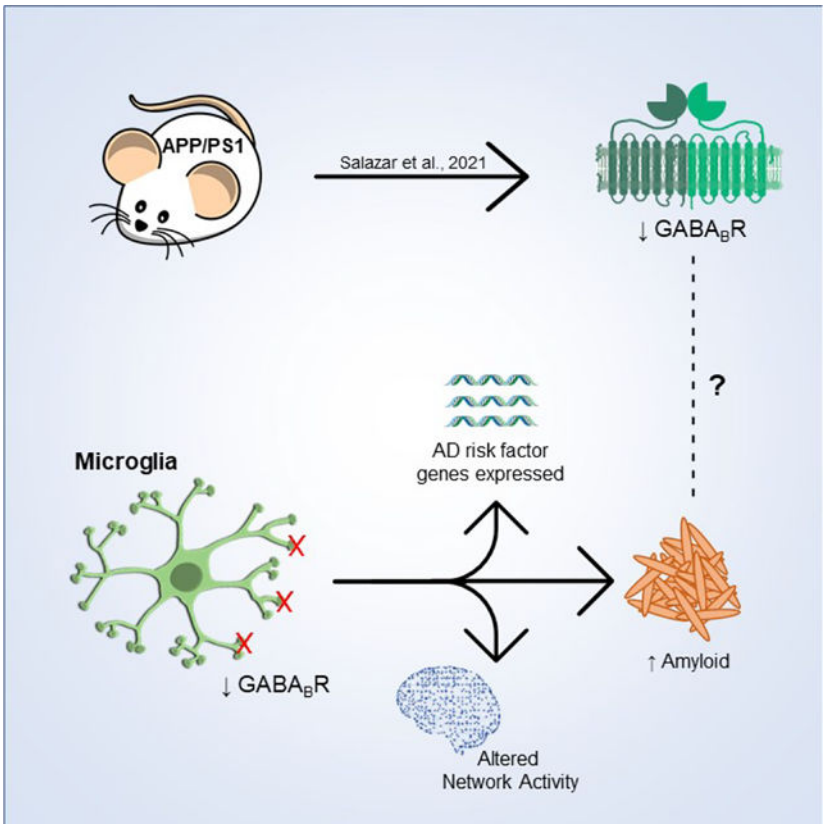

Keywords

Alzheimer's Disease; Glia; Amyloid; GABABR; NanoString; Electrophysiology; Flow Cytometry; Mouse models

1. Introduction

Currently, it is estimated that 6.2 million Americans are living with Alzheimer's Disease (AD) and while many other major causes of death have decreased (i.e. heart disease, HIV), the number of AD cases have increased 145.2% between 2000 and 2019, and this number will continue to rise (Alzheimer's Association 2021). Pathologically, AD is characterized by three core hallmarks: senile plaques composed of amyloid beta (Aβ), neurofibrillary tangles comprised of hyperphosphorylated tau (pTau), and chronic inflammation (neuroinflammation). Aβ plaques are derived from amyloid precursor protein (APP), which belong to a family of proteins involved in nervous system development, synaptic plasticity, learning and memory, and neuroprotection (Müller et al., 2017).These amyloid peptides bond together, forming extracellular Aβ plaques, leading to disruption of cellular communication, synaptic toxicity, alterations in receptor activation and cellular pathways, and promote the release of pro-inflammatory proteins and neurotoxins (Yankner & Lu, 2009). Neurofibrillary tangles of pTau are another AD pathology that more closely correlates to severity of the disease (Hanseeuw et al., 2019; La Joie et al., 2020). In AD, tau becomes hyperphosphorylated and cannot return to their stabilizing position, leading to

the collapse of microtubules, disrupting the cellular processes and, eventually, leading to neuronal cell death (Ballatore et al., 2007; Mandelkow & Mandelkow, 1998; Medeiros et al., 2010).

The investigation of the first two core pathologies in AD in animal model systems has primarily focused on genetic alterations observed in familial AD (fAD) that account for 1–3% of all AD cases. These include investigations of amyloid pathogenesis via mutations in the *App* gene, along with presenilin 1 (*Psen1*) and presenilin 2 (*Psen2*) genes, that develop Aβ plaques (e.g. APP/PS1 mice) (A. Salazar et al., 2019). Similar investigations in tau mouse models have been utilized to explore pathogenic mechanisms of tau in AD (Bellucci et al., 2004; Dumont et al., 2011; Jiang et al., 2016; Koller et al., 2020; A. Salazar et al., 2019). This approach has provided substantial insight into the underlying biology of AD, however, the identification of preclinical models that have relevance to late-onset AD (LOAD) and do not rely on fAD mutations is needed. More recent investigations of immune function and interactions of immune signaling and genes altered in the more common LOAD have shown promise (Guerreiro et al., 2013; Jay et al., 2017). The identification of mechanisms driving the pathology and/or associated with amyloid or tau pathogenesis without reliance on fAD mutations is needed to understand LOAD. Given substantial data demonstrating altered glial function contributes to both Aβ and tau pathology, this has become a productive target (S. E. Hickman et al., 2008; Kinney et al., 2018; Krabbe et al., 2013; Mandrekar & Landreth, 2010; Perea et al., 2018).

Neuroinflammation is fundamental in the central nervous system (CNS) as a protective mechanism to ensure adaptive brain function and response to insult. The response is attributed to the activation of macrophages, in particular microglia, which are essential in the maintenance of a healthy environment, however, in diseased states, they can become chronically activated (Lull & Block, 2010; Tremblay et al., 2011). In AD, microglia attempt to rid the brain of Aβ through phagocytosis and degradation that has been shown to be beneficial in early stages of the disease in animal models (S. E. Hickman et al., 2008). However, through the progression of the disease, microglia become dysfunctional and lose the ability to clear Aβ, resulting in increased levels of Aβ accumulation (S. E. Hickman et al., 2008; Krabbe et al., 2013). This cycle of microgliosis, with an imbalance of pro-inflammatory and anti-inflammatory cytokines, results in a positive feedback loop that leads to chronic neuroinflammation, damaged neurons, and ultimately neurodegeneration (Giulian et al., 1994; Hammond et al., 2019; S. Hickman et al., 2018; Z. Liu et al., 2019; Streit et al., 1999). In AD, microgliosis exacerbates the pathogenesis of the disease, increasing the production of Aβ and pTau, while in turn, these pathologies continue to drive neuroinflammation (S. E. Hickman et al., 2008; Mandrekar & Landreth, 2010; Meda et al., 1995; Perea et al., 2018; Sheng et al., 1998; Španić et al., 2019; Talan, 2019).

The above interaction of glia and AD pathophysiology has shifted considerable focus to glial regulation in AD, as well as approaches to intervene in microgliosis as a therapeutic target (See review Xu et al., 2016). The investigation of immune regulation in AD has spanned considerable targets that range from the role of various cytokines (Alam et al., 2016; Sawada et al., 2006; Smith et al., 2012; Yang et al., 2017) to microglial activation and morphology (Dubbelaar et al., 2018; Navarro et al., 2018), as well as the role of

discrete receptors expressed on glia and their involvement in regulation of inflammation (Angelopoulou et al., 2020; Ardestani et al., 2017; González-Scarano & Baltuch, 1999; Haque et al., 2018; King et al., 2017; J. Y. Lee et al., 2006; B. Liu & Hong, 2003). Given the extensive glial and neuronal interactions, the receptor assemblies regulating glia function are vital to understand, in particular as it is related to AD, during which loss of numerous transmitter and receptor systems are observed. Of relevance, are the G protein-coupled receptors (GPCR) that serve roles in regulation of both neuronal and glial function.

The gamma-aminobutyric acid receptor B ($GABA_B$), a metabotropic, $G_{i/o}$, represents a novel target for evaluation of GPCR activity and glial function. Considerable data has been published describing neuronal $GABA_B$ and its role in regulating neuronal inhibition (Gassmann & Bettler, 2012; Kantamneni, 2015; Shen et al., 2017), network function (Benarroch, 2012; Gaiarsa et al., 2011; Kohl & Paulsen, 2010), and learning and memory (Heaney & Kinney, 2016; M. Lee, Schwab, et al., 2011). More recently, data have demonstrated $GABA_B$ is expressed on microglia and serve a role in regulating immune response (Charles et al., 2003; Crowley et al., 2015; Kuhn et al., 2004; M. Lee, Schwab, et al., 2011). $GABA_B$ is composed of two different subunits, $GABA_{B1}$, consisting of the ligand binding site, and $GABA_{B2}$, the G-protein binding domain, responsible for evoking changes in cellular function (Biermann et al., 2010; Marshall et al., 1999). There are two different types of $GABA_{B1}$ subunits, $GABA_{B1a}$ and $GABA_{B1b}$; though similar in most ways, $GABA_{B1a}$ has two additional short consensus repeats, or sushi domains (SD) (Bettler et al., 2004; Hawrot Edward et al., 1998). As it relates to AD, recent data have demonstrated an interaction of the SD of $GABA_B$ with soluble APP that alters neuronal excitability (Rice et al., 2019). The SD also influences trafficking of B1 isoforms based on the presence or absence of these SDs in neuronal organization, though their interactions with specific proteins in glia may also be involved in trafficking (Biermann et al., 2010; Blein et al., 2000; Guetg et al., 2009; Hannan et al., 2012). While the literature on glial $GABA_B$ is limited, some evidence demonstrates $GABA_B$ inhibition of pro-inflammatory cytokines, IL-6 and TNF-α, during GABA activation, as well as attenuation of intracellular inflammatory mediator, NF-κB (M. Lee, Schwab, et al., 2011). Given additional literature demonstrates that astrocytes manufacture and release GABA, especially during a reactive state (Ishibashi et al., 2019; Jo et al., 2014; Le Meur et al., 2012; M. Lee, McGeer, et al., 2011) and the lack of any data indicating other GABAergic receptors on glia, this receptor likely serves a role in astrocyte mediated regulation of glia.

In patients with AD, there has been evidence of alterations in GABAergic signaling that may contribute to the disease (Y. Li et al., 2016; A. M. Salazar et al., 2021) and between the relationship of $GABA_B$ and inflammation, the impact of the $GABA_B$ receptor on the immune response and disease progression merits investigation. We have recently reported that at 6 months of age, male APP/PS1 mice demonstrated a significant decrease in all three $GABA_B$ receptor subunits, $GABA_{B1a}$, $GABA_{B1b}$, and $GABA_{B2}$, in both mRNA and protein, though this was not observed in 4-month-old APP/PS1 mice (A. M. Salazar et al., 2021). These findings indicate that elevated amounts of amyloid at 6 months of age lead to a significant decrease in the $GABA_B$ receptor in APP/PS1 mice (A. M. Salazar et al., 2021). With $GABA_B$ receptors found on both neurons and glia, we aimed to expand our investigation into the role of $GABA_B$ receptors specifically on glia, and the impact on glial

function in AD. We developed a mouse model, known as GAB/CX3ert, in which a reduction of $GABA_{B1a}$ subunit exists on macrophage populations by use of the Cre-loxP system. In addition, a yellow florescence protein gene (YFP) was inserted into the genome to express as an indicator of recombination. Interestingly, the crossbreeding of these models was also recently reported by another group in which the study focused on assessing microglial and neuronal communication during development (Favuzzi et al., 2021), whereas our study aims to evaluate AD relevant differences.

In this study, we demonstrated a knockdown of the $GABA_BR$ through flow cytometry in our GAB/CX3ert mouse model. We investigated if alterations in glial $GABA_B$ resulted in any AD relevant changes given our previous data. This included electrophysiological characterization, as well as expression of mouse transcripts, via NanoString technologies, comparing the GAB/CX3ert model to the fAD APP/PS1 mouse model, and to human AD risk genes. We further examined the role of glial $GABA_B$ in AD pathology by crossing the $GABA_B$ knockdown mice with the APP/PS1 model (GAB/CX3ert x APP/PS1) and examined the same risk genes, as well as amyloid pathology. Quantification of Aβ was performed through Luminex multiplex assay to compare the amount of Aβ present in the GAB/CX3ert x APP/PS1 compared to the APP/PS1 mice. To our knowledge, this is the first study to use a mouse model exhibiting $GABA_B$ loss, specifically on macrophages, in AD research to assess the relationship to disease-related changes.

2. Materials and Methods

2.1. Animals

2.1.1. Development of GAB/CX3ert Mice and Breeding of GAB/CX3ert x APP/PS1—

The novel mouse model, GAB/CX3ert, was developed by crossing the *Cx3cr1*^{CreER} mouse model (Dr. Dan Littman, Jackson Laboratory, B6.129P2(Cg)-C*x3cr1*$^{tm2.1(cre/ERT2)Litt}$/WganJ) with a $GABA_{B1a}$ knockout mouse, $GABA_{B1}$-eGFP, generously donated by Dr. Bernhard Bettler (Casanova et al., 2009; Haller et al., 2004). *The* $GABA_{B1}$-eGFP, containing the sequence for Cre recombinase and lox-P, was bred with the *Cx3cr1*^{CreER} mouse model for development of the novel GAB/CX3ert model. The model is designed to knockdown the $GABA_{B1a}$ receptor subunit, restricted to macrophages, with yellow fluorescent protein (YFP) reporter expressed as indictor of recombination. The GAB/CX3ert model was developed to utilize a drug, tamoxifen (TAM), as the Cre recombinase activator. During our investigations, we found no significant effects of TAM on the quantity of GABABR or YFP levels. To avoid drug effects of using TAM on the mice, we opted out of using TAM during this study, though demonstrate alterations in GABABR occurring spontaneously, as previously described by others using the *Cx3cr1*^{CreER} mouse model (Álvarez-Aznar et al., 2020; Fonseca et al., 2017; Kristianto et al., 2017; Zhao et al., 2019).

2.1.2. Genotyping—

For verification of genetics, isolation of genomic DNA from tail samples was used for genotyping by polymerase chain reaction (PCR). Evaluation of the $GABA_{B1}$ flox transgene was performed using (forward) 5’- CGC TTA TCG AGC AGC TAC AG -3’ and (reverse) 5’- ACC TTT CAA CCC AGC CTC AG -3’primers (Integrates

DNA Technologies, Coralville, Iowa). The mutant gene produces a band size of 540 bp or the WT gene product, with a band size of 325 bp. CX3cr1 transgene genotyping was performed using common primer (forward) 5'- AAG ACT CAC GTG GAC CTG CT -3', mutant primer (reverse) 5'- CGG TTA TTC AAC TTG CAC CA -3', and wildtype primer (reverse) 5'- AGG ATG TTG ACT TCC GAG TTG -3' (Integrates DNA Technologies, Coralville, Iowa). The mutant gene yields a 300 bp product or a WT band of 695 bp. The mice are maintained as a homozygous colony and majority of mice bred test positive for both mutant genes. Only mice that tested positive for both mutant genes were used in the completion of this study.

APP/PS1 mice were purchased through The Jackson Laboratory (B6.Cg-Tg(APPswe,PSEN1dE9)85Dbo/Mmjax) and maintained as a heterozygous colony per breeding considerations (male hemizygous APP/PS1 mice were breed with female C57BL/6J). Genotyping was also performed through isolation of genomic DNA from tail samples by PCR. The APP 397bp transgene was determined using (forward) 5'- AGG ACT GAC CAC TCG ACC AG -3' and (reverse) 5'- CGG GGG TCT AGT TCT GCA T -3'. The PS1 gene, 608bp in size, was also evaluated through (forward) 5'- AAT AGA GAA CGG CAG GAG CA -3' and (reverse) 5'- GCC ATG AGG GCA CTA ATC AT -3'primers. Wildtype control genes were also present using primers (forward) 5' – CTA GGC CAC AGA ATT GAA AGA TCT - 3'and (reverse) 5' – GTA GGT GGA AAT TCT AGC ATC ATC C – 3', with a size of 324bp. Mice that did not test positive for both the APP and PS1 genes were not used during this study.

GAB/CX3ert x APP/PS1 mice were bred by pairing male hemizygous APP/PS1 mice with female homozygous GAB/CX3ert mice. Tail samples were acquired and used for isolation of genomic DNA and PCR. Mice were tested for all four genes ($GABA_{B1}$ flox gene, and CX3cr1, APP, and PS1 transgenes). Only mice that tested positive for all four mutant genes were used in the completion of the study.

2.1.3. Care of Animals—C57BL/6J, GAB/CX3ert, APP/PS1, and GAB/CX3ert x APP/PS1 mice were used in the completion of this study. Mice were 6 months of age for all studies except the Luminex multiplex evaluation of Aβ, in which an aged group of 14-month-old mice were used. All animals were group-housed with a 12–12-hour light–dark cycle, with food and water available *ad libitum*. Animals were handled once per week to reduce stress and anxiety (Hurst & West, 2010). All procedures were performed during the light phase and in accordance with the University of Nevada, Las Vegas Animal Care and Use Committee and NIH guidelines for ethical treatment of research subjects.

2.1.4. Behavioral Screen—To evaluate the general health and neurological reflexes of the novel GAB/CX3ert mice, animals were assessed by using a modified standard behavioral screen as previously described (Crawley, 1999; Murtishaw et al., 2018; Wrenn et al., 2004). Fur condition, whisker condition, body tone, and limb tone were evaluated to determine the general health. Positional passivity, truck curl, forepaw reach, righting reflex, and wire hang were also evaluated for motoric abilities. To determine neurological reflexes, eye blink, pinna twitch, vibrissae response, toe pinch, and visual cliff were assessed. Assessment of behavioral reactivity was performed through attempted escape, struggling and vocalization

during handling, and dowel biting. Using an empty cage, mice were scored for transfer freezing, wild running, stereotypies, exploration, and grooming. Nociception was evaluated by measurement of latency to flick their tail away from hot water (55°C).

2.2. Flow Cytometry

Mice were sacrificed via Somnasol (Henry Schein Animal Health, Dublin, Ohio) intraperitoneal injection, transcardially perfused with 20mL sterile 1x PBS, and decapitated. Brains were removed and placed in a tube of sterile 1x PBS on ice and immediately processed for flow cytometry. Brains were mechanically homogenized and digested using Neural Tissue Dissociation Kit (Cat. No. 130–092-628 (Kit P), Miltenyi Biotec, Auburn, California) per manufacture guidelines. Cell suspension was pipetted over a 70um cell strainer and HBSS with calcium was added. The samples were centrifuged, and supernatant was removed and discarded. The pellet was resuspended in 70% isotonic percoll dilution and 50% isotonic percoll dilution, 35% isotonic percoll dilution, and DPBS were layered respectively as described in a recent protocol by Agalave et al. (Agalave et al., 2020). Using differential centrifugation, microglia layers were isolated in a clean tube. Samples were again centrifuged, and supernatant was discarded. The pellet was resuspended in FACS buffer. A small sample of cells were stained with Trypan Blue and counted using the TC20 Automated Cell Counter (Bio-Rad, Hercules, California). A small portion of each sample was combined and used for fluorescence-minus-one (FMO) controls. Cells were blocked using FcR Blocking Reagent (mouse) (Miltenyi Biotec Cat. No. 130-092-575) The samples were probed with primary antibodies [Primary antibodies: Anti-$GABA_{B1}$ unconjugated (Cat. No. ab55051, Abcam, Cambridge, Massachusetts), Anti-CD11b APC (Cat. No. 1106055, Sony, New York, New York), Anti-$GABA_{B2}$ AF700 (Cat. No. NBP2-59335, Novus Biologicals, Littleton, Colorado), Anti-CD45 PE/Cy7 (Cat. No. 115565, Sony, New York, New York)] in the dark for one hour. Cells were rinsed twice, and secondary antibodies were added for the target $GABA_{B1}$ [Secondary antibody: PE Texas Red (Cat. No. M32017, Invitrogen, Carlsbad, California)] for 30 minutes. Cells were again rinsed and resuspended in FACS buffer.

Samples were analyzed using the Sony SH800S Cell Sorter (Sony, New York, New York). Compensation was performed using UltraComp eBeads Compensation Beads (Invitrogen Cat. No. 01-2222-41). No viability dye was included, due to previous data demonstrating the use to be unnecessary in this samples and allowing for greater number of channels used for protein targets. Doublet discrimination was performed by plotting the cell width by area to ensure the analysis of only single cells (Figure S1), and targets were gated using FMOs controls. Gating strategy first identified macrophages through $CD11b^+/CD45^+$ cells, then evaluated the percent of $GABA_{B1}{}^+$, $GABA_{B2}{}^+$, and YFP^+ from the parent population. A minimum of 250,000 events analyzed per animal, consistent with previous studies (Hu et al., 2021; McQuade et al., 2020; Nava Catorce et al., 2021). Data was analyzed via SPSS statistical software version 25 (IBM, Armonk, New York) for one-way ANOVA values to determine significance between GAB/CX3ert mice and controls.

2.3. Luminex Multiplex Immunoassay

2.3.1. Protein Extraction—For collection of brain tissue, mice were individually euthanized by an i.p. injection of Somnasol (Henry Schein Animal Health, Dublin, Ohio). Mice were transcardially perfused with 20mL sterile 1x PBS and decapitated. Brains were removed and dissected for hippocampus, cortex, and cerebellum, for both right and left hemispheres. Tissues were flash frozen with liquid nitrogen and stored in −80°C until protein isolation. Whole protein lysates were extracted from frozen hippocampal tissue using Bio-Plex Cell Lysis Kit (Cat. No. 171304011, Bio-rad, Hercules, California) following manufacturer's protocol, consistent with a recent 2022 study using Luminex assays (Pillon et al., 2022). Complete cell lysis buffer was added to the frozen tissues, homogenized (Kinematica Polytron 1300D, Luzern, CHE), and incubated overnight at −80°C. The following day, the homogenates were allowed to thaw on ice and immediately sonicated (Branson SFX 150, Branson Ultrasonics, Brookfield, Connecticut). The samples were centrifuged for 10 minutes at 4,500g. Supernatants were transferred to a new, low-binding centrifuge tube. Total protein concentrations were measured using Pierce Bicinchoninic Assay Kit (Cat. No. 23255, Thermo Fisher Scientific, Waltham, Massachusetts) per the manufacturer's protocol. Prior to storage, protein lysates were diluted to the highest, consistent concentration of 200,000ug/μL with complete cell lysis buffer, to facilitate equal volume protein loading. Lysates and dilutions were stored at −80°C until use.

2.3.2. Luminex Data Collection—Milliplex Mouse Amyloid Beta Magnetic Bead Panel (Millipore Sigma, Cat. No. MABMAG-83K) was used to quantify AB-40 and AB-42 levels in the hippocampal tissue from the mouse models. Standards were prepared in Assay Buffer provided by the kit. Samples were prepared and assay was performed per the manufacture's protocol without modifications. Concentrations were determined by simultaneously evaluated AB-40 and AB-42 using Luminex multiplex immunoassay (Bio-Plex 200 system, Bio-Rad, Hercules, California). Raw data was exported and statistically analyzed using SPSS statistical software version 25 (IBM, Armonk, New York) and one-way ANOVA was performed to determine statistical values, reaching statistically significance of $p < 0.05$.

2.4. Immunohistochemistry

Whole brains in 1x sterile PBS with 0.05% sodium azide were rinsed with 1x PBS for 5 minutes and froze in −20 °C for 15 minutes. Brains were mounted to cryostat chuck using a tissue freezing medium (Cryostat Microtome CF-6100, Precisionary, Natick, MA). Thirtymicron sections were generated and kept in 1x PBS at 4 °C until use. Briefly, the sections were blocked in 1x PBS with 0.3% Triton-X and 10% fetal bovine serum (FBS, Cat. No. 89510–194, VWR, PA, USA) overnight, at 4 °C overnight with gentle shaking, and subsequently incubated with primary antibody mixture for 2 hours (1x PBS with 0.1% Triton-X, 10% FBS, 1:1000 Iba1 (Cat. No. 019-19741), Wako, CA, USA). The sections were rinsed with 1x PBS with 0.3% Triton-X, 3 times for 10 minutes each, with gentle shaking and incubated with secondary antibody mixture 45 minutes, at RT with gentle shaking (1x PBS with 0.1% Triton-X, 10% FBS, 1:1000 Alexa Fluor 594 (Cat. No. A11012), Invitrogen, Waltham, MA, USA). The sections were rinsed with 1x PBS with 0.3% Triton-X, 3 times for 10 minutes each and additional wash in 1x PBS 2 times for

10 minutes each, with gentle shaking. Staining for Aβ followed using 0.05% Thioflavin S (Cat. No. T1892, Millipore-Sigma, MO, USA) dissolved in 50% ethanol. The sections were incubated for 8 minutes, followed by 2 rounds of differentiation in 80% ethanol for 10s each. The sections were rinsed in a generous amount of sterile distilled water 3 times and transferred in cold 1x PBS before slide mounting. Poly-L-Lysine–coated slides (Cat. No. 63410-01, Electron Microscopy Sciences, PA, USA) were used to mount sections. Fluoromount G (Cat. No. 17984, Electron Microscopy Sciences, PA, USA) was added onto sections before covering with glass slip and allowed to dry for at least 10 minutes at 4 °C, followed by sealing the edges with clear nail polish. Mounted sections were kept at 4 °C until imaging. Florescence microscopy was conducted using ECHO florescence microscope (San Diego, CA).

2.5. Electrophysiology Experiments

2.5.1 Surgical Procedures—Fifteen male mice (C57BL/6J = 5; GABA/CX3ert = 5; APP/PS1 = 5) aged eight to twelve months (twenty-five grams - thirty-four grams) were implanted with a fixed recording array containing eight tetrodes. Four tetrodes targeted the medial frontal cortex (area 32 - ACC (anterior 1.0 mm, lateral 0.3 mm from bregma, dorsoventral 0.8 mm) and four targeted the ipsilateral dorsal CA1 (posterior 2.2 mm, lateral 1.6 mm from bregma, dorsoventral 1.2 mm). Coordinates were taken from Paxinos and Franklin (2019), and the location of recording wires was confirmed using electrophysiological markers (Buzsáki, 1986). A ground electrode was placed in the contralateral cerebellum and soldered to the electrode interface board (EIB; Plexon Inc. Dallas, Tx) on the recording array. Three screws were placed along the cranial ridge, and dental acrylic was used to affix the array to the skull. Following surgery, mice were housed individually on a twelve-hour light-dark cycle with food and water available *ad libitum* and received one injection per day of Enroflox (0.01 ml/g; Bayer, Leverkusen, Germany) and Rimadyl (0.01 ml/g; Pizer, New York, NY) for seven days after surgery before electrophysiological recordings occurred.

2.5.2 Electrophysiological Recordings—Subjects were habituated to two neutral (no rewarding or aversive stimuli presented) recording chambers prior to electrophysiological recordings. The chambers were contextually unique but sized similarly (~sixty cm long and forty-five cm long, the walls were forty-five cm tall). The affixed recording array was attached to a headstage (Intan Technologies, Los Angeles, CA) and digitized electrophysiological signals were sent through tether cables into an RHD 2000 USB interface board (Intan Technologies). Local field potentials (LFPs) were sampled at thirty kHz and bandpass filtered between 1–6000 Hz with the Open Ephys GUI (V0.5.0, Cambridge, MA). Behavior was tracked using Bonsai (Lopes et al., 2015). Running speed was calculated distance over time (ms). Running speed between groups was examined using a one-way ANOVA and second by second behavioral states were grouped using unsupervised learning (kmeans clustering; Python V3.7, Scikit Learn) to identify still or slow, walking, or running states.

2.5.3. Electrophysiological Data Analysis—LFP data were read into a computer workstation for data preprocessing. LFP data were downsampled to 1000 Hz and then notch

filtered between 58–61 Hz to remove 60 cycle noise signal. Noisy signals were removed by visual inspection and one wire from each tetrode was selected to reduce redundancy in data analysis. All electrophysiological data were preprocessed using custom code written in Python V3.7.

In the current experiments, we were interested in electrophysiological activity during active behavioral periods. Our exposures were in 10-minute blocks, it was possible that some animals fell asleep in that period, while others did not, which might have skewed our SWR findings. SWRs are more frequent during sleep than waking periods (Joo & Frank, 2018). To avoid including possible sleep episodes in SWR analysis, we identified any periods when animals were still for >30 subsequent seconds. In total, we found 13 events across all animals, sessions, and environments. All 13 of these events occurred during the second half of exposures in both environments, thus we limited all our electrophysiological analyses to only the first 300s of exploration in each environment.

2.5.4. Sharp-wave Ripple Detection—Sharp-wave ripple (SWR) detection was accomplished using the freely available Kay Ripple detector (Kay et al., 2016). Briefly, hippocampal LFPs were bandpass filtered between 150 – 250 Hz. The filtered envelope was identified using the Hilbert transform and SWR amplitude was Gaussian filtered with four milliseconds bins and four milliseconds overlap. Detected events greater than 2.0 standard deviations above the mean that persisted for more than 15 milliseconds were classified as SWR events. We calculated behavior by SWR event using decoded behavioral states (discussed above). If the animal was in the still when the SWR occurred, it was identified as an immobile SWR otherwise it was classified as walking or running.

2.5.5. Statistical Analysis—Unless otherwise stated, all electrophysiological statistical analysis was performed in Python (V3.7) using *statsmodels* (V0.13). Subject mean value for each measure so that each subject reported one data point in all statistical tests. We utilized a group model to compare the main effects for each electrophysiological measure. Pairwise Tukey HSD module from *statsmodels* (V0.13) was applied to significant main effects for post hoc comparisons between groups.

2.6. NanoString

2.6.1. Total RNA Isolation—Mice were euthanized by an i.p. injection of Somnasol (Henry Schein Animal Health, Dublin, Ohio). Mice were transcardially perfused with 20mL sterile 1x PBS and decapitated. Hemibrains were removed and flash frozen immediately with liquid nitrogen. Samples were placed into −80 degrees Celsius until processed. To perform RNA isolation, brains were kept frozen while homogenized. Samples were placed into clean tubes and RNeasy Lipid Tissue Mini Kit (Qiagen Cat. No. 74804) was used per the manufacture's protocol without modifications. For NanoString nCounter analysis, Alzheimer's Disease panel was used (NanoString Technologies, Seattle, WA, USA). Two hundred nanograms of RNA was loaded and was hybridized with probes for 16 h at 65 degrees C. The results obtained from the nCounter MAX Analysis System (NanoString Technologies, catalog #NCT-SYST-LS, Seattle WA) were imported into the nSolver Analysis Software (v4.0; NanoString Technologies) for QC verification,

normalization, and data statistical analysis using Advanced Analysis software (v2.0.115; NanoString Technologies). All assays were performed according to the manufacturer's protocols (PMID:33003412).

2.6.2. NanoString gene expression panel and data collection—The NanoString Mouse AD gene expression panel (Preuss et al., 2020) was used for gene expression profiling on the nCounter platform (NanoString, Seattle, WA). Mouse NanoString data was collected from brain hemispheres from six months old male mice. nSolver software was used for generating NanoString gene expression counts. Normalization was done by dividing counts within a lane by geometric mean of the housekeeping genes from the same lane. Next, normalized count values were log-transformed for downstream analysis.

2.6.3. AMP-AD post-mortem brain cohorts and gene co-expression modules —Data on the 30 human AMP-AD (Accelerating Medicines Partnership in Alzheimer's Disease) co-expression modules was obtained from the Synapse data repository (Allen et al., 2016; Mostafavi et al., 2018; Wang et al., 2018) (https://www.synapse.org/#!Synapse:syn11932957/tables/; SynapseID: syn11932957).

These 30 human AMP-AD modules were further grouped into five consensus clusters that describe the major functional groups of alterations observed in human AD (Preuss et al., 2020; Wan et al., 2020). A detailed description on how co-expression modules were identified can be found in the recent study that identified the harmonized human co-expression modules as part of transcriptome wide AD meta-analysis (Wan et al., 2020).

2.6.4. Comparison between mouse models—Differential gene expression analysis for each mouse model compared to the control strain (C57BL/6J) was performed using the voom-limma (Ritchie et al., 2015) package in R. Pearson correlations of gene expression changes (log fold changes versus control for each gene) were computed for each pair of mouse models and regression lines were fitted with the ggscatter package in R.

2.6.5 Gene set enrichment analysis—Gene set enrichment analysis (GSEA) (Subramanian et al., 2005) was performed using the clusterProfiler package (Wu et al., 2021) in the R software environment for the Kyoto Encyclopedia of Genes and Genomes (KEGG) database. Briefly, NanoString AD panel genes were ranked based on log fold change values obtained from differential expression analysis of each model. Enrichment scores for KEGG pathways were computed to compare relative expression on the pathway level between each mouse model.

2.6.6. Mouse-human expression comparison—To compare mouse expression changes with those observed in human disease, we computed Pearson correlations between changes in expression (log fold change) of each gene in a given AMP-AD module with each mouse model (Pandey et al., 2019; Preuss et al., 2020). Correlation coefficients were computed using cor.test function built in R as:

$$\mathrm{cor.test}(\mathrm{LogFC(h)}, \mathrm{LogFC(m)}) \quad (1)$$

where LogFC(h) is the log fold change in transcript expression of human AD patients compared to control patients, and LogFC(m) is the log fold change in expression of mouse transcripts compare to control (C57BL/6J). LogFC values for human transcripts were obtained via the AMP-AD knowledge portal (https://www.synapse.org/#!Synapse:syn11180450).

3. Results

3.1. Male GAB/CX3ert mice have decreased $GABA_B$ receptor subunits on macrophages

To verify genetic recombination in the GAB/CX3ert mouse model, and assessment of $GABA_B$ subunit loss on macrophages, flow cytometry was utilized for evaluation of whole-brain cell suspension. Cells were labelled with CD11b and CD45, a co-positive marker of macrophages, and were evaluated for the $GABA_B$ receptor subunits. GAB/CX3ert male mice demonstrated a 54% decrease in $GABA_{B1}$ receptor subunit on macrophages compared to controls and a 58% decrease in the $GABA_{B2}$ receptor subunit (Figure 1B; $F_{1,6} = 31.342$, $p = 0.003$; $F_{1,6} = 9.007$, $p = 0.030$, respectively), with no difference in the overall number of macrophages between the two genotypes (Figure 1B; $F_{1,6} = 0.077$, $p = 0.792$). YFP was also evaluated as an indicator of recombination and showed that 36% of $CD11b^+/CD45^+$ cells expressed YFP (Figure 1C; $F_{1,6} = 315.316$, $p = 0.000$). Female GAB/CX3ert mice were also evaluated for the $GABA_B$ receptor, however, they did not show changes in $GABA_{B1}$ or $GABA_{B2}$ on macrophages (Figure 2B; $F_{1,6} = 2.302$, $p = 0.180$; $F_{1,6} = 1.388$, $p = 0.283$; respectively). There was an increase in YFP, indicating some recombination was occurring, though only 16% of macrophages expressed YFP (Figure 2C; $F_{1,6} = 72.447$, $p = 0.000$).

To assess any phenotypic differences in the general health of the mice, we performed a behavioral screen to progressively investigate any alterations in neurological reflexes, motoric abilities, behavioral reactivity, empty cage behavior, and nociception of GAB/CX3ert mice compared to wildtype controls. The evaluation resulted in no significant differences in any of the measures between the GAB/CX3ert and controls, in either male or female mice (Supplemental Figure 2). Overall, the GAB/CX3ert mouse model mutation resulted in a significant decrease in the $GABA_B$ receptor on macrophages in male mice, though did not result in variation in health or general behavior of the mice.

3.2. Altered Sharp-Wave Ripple activity in GABA/CX3ert and APP/PS1 Mice

The hippocampus (HC) is crucial for learning and memory processes and is one of the most affected regions of the brain in AD, contributing to the clinical manifestation of the disease. Hippocampal sharp-wave ripple (SWR) activity is thought to stabilize newly learned hippocampal traces and is an essential mechanism for consolidating these traces to the cortex and other areas (Buzsáki, 2015). Disruption of SWR activity profoundly impairs learning and memory (Caccavano et al., 2020; Ego-Stengel & Wilson, 2010, p.). To this end, we investigated if a reduction of the $GABA_BR$ on macrophages could lead to alterations in hippocampal SWR activity, as well as compare the changes to a well-established amyloid model of AD.

We compared the number of SWRs per second during environmental exploration of C57BL/6J, GAB/CX3ert, and APP/PS1 mice. GAB/CX3ert and APP/PS1 mice had significantly fewer SWRs than controls (Figure 3A and 3B). A one-way ANOVA revealed significant group main effects ($F_{(2, 12)} = 5.83$, p = 0.017), and post hoc tests showed that both GAB/CX3ert (p = 0.04) and APP/PS1 (p = 0.02) were significantly altered. We found no differences in SWR peak frequency between groups (p=0.54; Figure 3B). We also found no differences in power at SWR peak power in the HC (p=0.626; Figure 3B), SWR duration (p=0.92; Figure 3B), and SWR amplitude (p=0.18; Figure 3B).

SWR activity has been linked with memory consolidation and is thought to be integral for strengthening memory traces outside the HC, thus, we also examined cortical activity during HC SWRs. Interestingly, we found that anterior cingulate cortex (ACC) SWR power at peak frequency was significantly decreased from controls ($F_{(2, 12)} = 6.56$) for both GAB/CX3ert (p = 0.01) and APP/PS1 (p = 0.04; Figure 3B) mice. Altered HC-cortical interactions during SWRs have been hypothesized to disrupt memory processing (Tang & Jadhav, 2019), and have been previously reported in APP/PS1 (Jura et al., 2019), so it is particularly notable that GAB/CX3ert mice are affected similarly. Overall, we found similar abnormalities in SWR activity in both GAB/CX3ert and APP/PS1 mice, in terms of a reduction in the total number of SWR events and in the spectral power of SWRs in the ACC. These effects suggest that the glial-specific loss of the $GABA_BR$ in the GAB/CX3ert mice are affecting hippocampal activity and hippocampal-cortical communication, as similarly observed in the amyloid model of AD.

3.3. ACC – Hippocampal Coherence is Disrupted in GABA/CX3ert Mice

With our results showing a decreased cortical response to hippocampal sharp waves in both APP/PS1 and GAB/CX3ert mice, we sought to further examine whether corticohippocampal interactions were affected more broadly, and, if again, there were similarities between GAB/CX3ert and APP/PS1 mice. We used ANOVAs to compare ACC-HC coherence between GAB/CX3ert, APP/PS1, and controls (Figure 3D) in delta (1–4Hz; Figure 3E), theta (5–12Hz; Figure 3F.), slow gamma (30–55Hz; Figure 3G), and fast gamma (62–120Hz; Figure 3H). We found that both GAB/CX3ert and APP/PS1 mice had significantly increased coherence in slow gamma ($F_{(2, 12)} = 5.63$, p = 0.011). Hypersynchrony in the slow gamma band indicates that network interactions between the ACC and HC were altered by the selective decrease in $GABA_BR$ on glial cells. In the delta band, APP/PS1 mice had elevated coherence from controls ($F_{(2, 12)} = 5.18$, p = 0.02), though no differences were found in the GAB/CX3ert mice when compared to the other genotypes (p > 0.05). In the analyzed periods here, there were no differences in spectral power found between groups in either delta, theta, beta, and slow or fast gamma power (p>0.05), suggesting that the coherence differences were not due to inherent differences in spectral power. Impairments in ACC-HC coherence in slow gamma band, along with the finding of reduced ACC SWR peak frequency power, suggests a wholesale impairment in communication between these areas. These effects indicate that the glial-specific changes found in the GAB/CX3ert mice are affecting hippocampal network activity and hippocampal-cortical communication.

3.4. Similar gene expression changes observed across all our mouse strains

Resemblance in the GAB/CX3ert and APP/PS1 mouse models in network activity led us to further evaluate the similarities in gene expression between the models, as well as the crossbred GAB/CX3ert x APP/PS1 mice. Using NanoString gene expression profiling of the three transgenic mouse models, we computed the log fold change in expression of mouse transcripts for each of the models compared to controls (C57BL/6J) (Supplemental_Tables_GeneExpressionChanges), followed by a correlation analysis using the change in expression values (logFC) for all 770 AD-related NanoString probes. We observed strong and significant correlation (Pearson correlation coefficient = 0.64, $p < 2.2 \times 10^{-16}$) between APP/PS1 and GAB/CX3ert mice (Figure 4A). Similarly, GAB/CX3ert x APP/PS1 mice showed strong positive correlation with both APP/PS1 (Pearson correlation coefficient = 0.61, $p < 2.2 \times 10^{-16}$) and GAB/CX3ert mice (Pearson correlation coefficient = 0.66, $p < 2.2 \times 10^{-16}$) (Figure 4B–C). Notably, we observed increased expression of mouse *App* gene in APP/PS1 transgenic mice (logFC = 0.60), but no significant changes in the GAB/CX3ert mice (logFC = −0.02). However, expression of the mouse *App* gene significantly increased in GAB/CX3ert x APP/PS1 mice compared to APP/PS1 (logFC = 0.27, FDR = 0.04), suggesting more pronounced effects in the double mutant than single variant model. Interestingly, despite the differences in *App* gene expression between the mutant strains, we observed overall very similar gene expression changes in the novel GAB/CX3ert mouse model as observed in APP/PS1 transgenic mice. Although these mutations are functionally very different (loss of the $GABA_BR$ on macrophages versus increased secretion of a human Aβ peptide with rare variants), these results demonstrate similar transcriptomic changes supported across almost all NanoString panel genes (Figure 4).

Next, we performed gene set enrichment analysis (GSEA) (Subramanian et al., 2005) in order to identify enriched pathways across each model. GSEA aggregates the per gene statistics across multiple pathways to identify transcriptional changes at the pathway level in a specific direction. We observed gene sets associated with multiple AD-specific processes were either upregulated or downregulated in all three mouse models (Supplementary Figure 3, Supplemental_Tables_GSEA). Multiple KEGG pathways such as oxidative phosphorylation and Alzheimer's disease were upregulated, while focal adhesion, endocytosis and signaling related pathways were downregulated in each mouse model (Supplementary Figure 3). In addition, we also observed multiple pathways that were either up- or down-regulated in specific mouse model, such as synaptic vesicle cycle, lysosome and osteoclast differentiation pathways were downregulated in APP/PS1 transgenic mice but upregulated in GAB/CX3ert and GAB/CX3ert x APP/PS1 mice (Supplementary Figure 3, Supplemental_Tables_GSEA). Altogether, the similarities in overall gene expression generally, but not universally, corresponded to pathway-level expression differences.

3.5. Mouse models reproduce human inflammation signatures in gene modules

In order to assess the relevance of our model for Alzheimer's disease, we performed a correlation analysis between our mouse NanoString data and human post-mortem co-expression modules (Preuss et al., 2020; Wan et al., 2020). Interestingly, all three groups of mice showed significant positive correlations ($p < 0.05$) with human co-expression modules in Consensus Cluster B, which include transcripts that are enriched for immune related

pathways in the superior temporal gyrus (STG) and the inferior frontal gyrus (IFG) brain regions (Figure 5A). Furthermore, all mouse strains showed significant negative correlations ($p < 0.05$) with the inferior frontal gyrus module (IFGblue in Consensus Cluster D), enriched for transcripts associated with cell cycle, RNA non-mediated decay, myelination, and glial development, implying that these processes are altered in the opposite direction than seen in endpoint Alzheimer's brains. Notably, GAB/CX3ert x APP/PS1 mice showed strong negative correlations ($p < 0.05$) with human co-expression modules in Consensus Cluster E, which are enriched for transcripts associated with organelle biogenesis and cellular stress response pathways across all brain regions (Figure 5A), while APP/PS1 and GAB/CX3ert mice showed significant negative correlations ($p < 0.05$) with human co-expression modules in the frontal pole (FP) and the parahippocampus gyrus (PHG) brain regions, also observed in Consensus Cluster E (Figure 5A). These effects are similar to those observed in the 5xFAD mouse model at six months of age (Oblak et al., 2021). These results represent opposite effects to those observed in endpoint Alzheimer's and, unlike the Consensus Cluster B and D results, are strengthened in the double mutant.

Furthermore, we identified genes driving significant positive correlations with immune related modules STGblue and IFGturquoise (Figure 5A) and found many common genes that were either upregulated (e.g. *C1qa*, *C1qb*, and *Tyrobp*) or downregulated (e.g. *Vav2* and *Zfp36*) in all three mouse models, similar to human Alzheimer's changes in STGblue (Figure 5B) and IFGturquoise (Figure 5C). Although the degree of change varied across these genes, as with *Trem2*, effects were generally consistent. Overall, we observed similar patterns when comparing each mouse model with disease-associated changes in human co-expression modules, suggesting decrease of the $GABA_BR$ on macrophages generates effects similar to APP/PS1 transgene in mice, significantly replicating effects in immune associated human modules.

3.5. Decrease of the $GABA_B$ receptor exacerbates Aβ pathology in GAB/CX3ert x APP/PS1 mice

As we reported above, NanoString investigations demonstrated increased expression of the *App* gene in the GAB/CX3ert x APP/PS1 mice. With this data, we aimed to evaluate how Aβ protein accumulation would be affected by this alteration of gene expression. To achieve this, we quantified the amount of Aβ-40 and Aβ-42 via Luminex multiplex assay. As expected, with no amyloid mutation present, minimal Aβ was detected in the C57BL6J and GAB/CX3ert mice (Supplemental Figure 4). Evaluation of Aβ between the GAB/CX3ert x APP/PS1 and APP/PS1 mice at 6 months of age demonstrated no significant differences in both males (Aβ-40: $F_{1,19} = 2.891$, $p = 0.106$; Aβ-42: $F_{1,19} = 0.713$, $p = 0.41$) and females (Aβ-40: $F_{1,19} = 0.763$, $p = 0.394$; Aβ-42: $F_{1,19} = 0.304$, $p = 0.588$; data not shown). It is noteworthy to mention that even though there were no significant differences, the male mice showed a positive trend of increased Aβ-40 and Aβ-42 in the double mutant compared to APP/PS1 mice alone at this timepoint.

With no significant changes in Aβ detected in the 6-month-old GAB/CX3ert x APP/PS1 mice compared to APP/PS1 mice of that age, we evaluated how aging may influence Aβ levels in a 14-month-old cohort of the genetically modified mice. This timepoint was chosen

to determine if aging impacts Aβ levels in the double mutant mice, with the idea that overall Aβ would not be too advanced to be undetectable, but allow investigates into whether the Aβ alterations attributed to the decrease of the GABA-BR emerge with age. We found that in male GAB/CX3ert x APP/PS1 mice there was a 49% increase in Aβ-40 and a 21% increase in Aβ-42, compared to the APP/PS1 mice (Figure 6A; $F_{1,19} = 7.793$, $p = 0.012$; $F_{1,19} = 5.434$, $p = 0.032$, respectively). Female GAB/CX3ert x APP/PS1 mice did not show a significant difference in the amount of Aβ-40 or Aβ-42 compared to APP/PS1 mice (Figure 6B; $F_{1,13} = 3.455$, $p = 0.088$; $F_{1,13} = 0.770$, $p = 0.770$, respectively), as this is consistent with the absent change in the $GABA_B$ receptor reported in female GAB/CX3ert mice.

Brains of the male GAB/CX3ert x APP/PS1 and APP/PS1 were evaluated via immunohistochemistry and demonstrated an increase in Aβ plaque number and size in several fields of the hippocampus, including dentate gyrus, consistent with significant increase in Luminex quantification (Supplemental Figure 5).

Our study demonstrated similar transcriptomic changes in the GAB/CX3ert and APP/PS1 mice, as well as an increased effect in the double mutant. Altogether, the reduction of the $GABA_B$ receptor in the males of the crossed model, GAB/CX3ert x APP/PS1, led to an increase in *App* gene expression and, furthermore, an increase in Aβ pathology compared to APP/PS1 alone; this supports the concept of more pronounced effects of the *App* gene in GAB/CX3ert x APP/PS1 mice. With our previously published work demonstrating a reduction in the $GABA_BR$ in the APP/PS1 amyloid model (A. M. Salazar et al., 2021), as well as our current finding of increased Aβ pathology in the GAB/CX3ert x APP/PS1 mice, these data together highlight the relationship between $GABA_BR$ loss and Aβ pathology.

4. Discussion

The GAB/CX3ert mouse model we developed has utility in investigating glia's influence on disease, as well as the role of $GABA_BR$. Specifically, we evaluated the GAB/CX3ert mice in relation to AD pathology and mechanisms. Flow cytometry validated the GAB/CX3ert model in males by demonstrating a 54% decrease of the $GABA_{B1}$ receptor subunit restricted to the macrophage population, as well as a similar significant decrease in the $GABA_{B2}$ subunit (58%), indicating a loss of functional receptors. There were no significant differences observed during evaluation of general health between the GAB/CX3ert and control mice. In addition, we report that the genetic mutation did not result in lethality, as previously described in the complete $GABA_{B1}$ knockout mouse models (Prosser et al., 2001; Quéva et al., 2003), demonstrating that survivability is not compromised by the loss of $GABA_B$ function on glia. This indicates that there are clear phenotypic differences between the two models depending on the specific cell type being altered. Our model demonstrated genetic recombination in the absence of tamoxifen, so tamoxifen was not used, as it seemed to be an unnecessary variable. Previous studies with tamoxifen described alterations in memory, locomotor activity, anxiety, and immobility during a swimming task, as well as depressive-like behavior (X. Li et al., 2020; D. Pandey et al., 2016; Wang et al., 2016). Genetic recombination without tamoxifen in our model is also consistent with other reports of cre-lox systems in genetically modified mice being "leaky", attributed to small amounts of cre entering the nucleus without induction from tamoxifen or active transport into the

nucleus (Chappell-Maor et al., 2020; Sahasrabuddhe & Ghosh, 2022; Van Hove et al., 2020). However, even with reports of “leaky” cre activity in the mouse models used in targeting microglial function, the CX3CR1-Cre ER models have contributed greatly to the field (Bruttger et al., 2015; Goldmann et al., 2013; Parkhurst et al., 2013; Sahasrabuddhe & Ghosh, 2022; Tay et al., 2017).

It is worth noting that another group recently published a similar novel mouse model (Favuzzi et al., 2021) in crossbreeding of the $GABA_{B1}$ floxed mice (Haller et al., 2004) and the B6.129P2(Cg)-Cx3cr1^{tm1Litt}/J model (Dr. Dan Littman, Jackson Laboratory), as we used for the development of the GAB/CX3ert mice. Consistent with our findings, their animals had no apparent overt deficits or survivability issues. The focus of the Favuzzi et al. (2021) study was on assessing microglial and neuronal communication during development as opposed to evaluation of AD relevant differences that we have observed in the present study.

With the hippocampus being one of the most affected brain regions in AD, hippocampal network activity is of considerable interest for studying dementia-related disorders (Fjell et al., 2014; Lok et al., 2013). Hippocampal sharp waves have been linked with memory formation, consolidation, and usage (Joo & Frank, 2018; Pfeiffer & Foster, 2013) and they have also been a mechanism of interest underlying memory dysfunction found in AD patients and animal models. Notably, multiple recent findings have shown that a range of AD animal models, including the foundational APP/PS1 model, have significant reductions in the frequency of SWR events (E. A. Jones et al., 2019; Jura et al., 2019). Here, we report that GAB/CX3ert mice also showed decreased SWR events, similar to APP/PS1 mice, suggesting that these animals may exhibit some form of long-term memory impairment. Furthermore, our results indicate that there is an important role for $GABA_BR$ on macrophages in normal hippocampal network function.

Communication by coherence is thought to be the principal mechanism that enables physically separated brain areas to work together (Fries, 2015). Local field potential coherence between the medial prefrontal cortex (including the ACC) and the HC has been linked to spatial processing (Zielinski et al., 2019), spatial working memory (M. W. Jones & Wilson, 2005), and memory recall (Makino et al., 2019; Wirt & Hyman, 2019). Prefrontal-hippocampal coherence is of great interest both as a diagnostic and therapeutic biomarker for a variety of psychiatric and neurodegenerative disorders (M. Li et al., 2015; Ranasinghe et al., 2020; Wirt et al., 2021) and is often impaired in transgenic mouse models of these disorders (Sigurdsson et al., 2010; Zhurakovskaya et al., 2019). While most effects have been found in the theta range, others have reported alterations in both delta (Schultheiss et al., 2020) and gamma (Bygrave et al., 2019). The GAB/CX3ert model showed increased coherence in slow gamma, as also observed in the APP/PS1 mice, indicating alterations in network interactions between the ACC and HC. Future experiments will be needed to understand how projection neurons between the ACC and HC and/or those traveling through thalamic relays are affected by partial depletion of $GABA_BR$ on glia. This may cause impairments in spatial working memory (Hallock et al., 2013) and memory recall (Davoodi et al., 2009; Ramanathan et al., 2018). The observed impairments

in communication between the ACC and HC suggest that GABA/CX3ert mice may have some form of learning and memory impairment not yet identified.

Analysis of gene expression through NanoString demonstrated the striking similarity between gene expression changes in the GAB/CX3ert and APP/PS1 mouse models, consistent across all genes and, to our knowledge, unique for a non-amyloidogenic model. Although the correspondence with human gene modules (Figure 6A) is similar to those observed in 5xFAD and other mice with mutant amyloid overexpression (Oblak et al., 2021; Wan et al., 2020), different patterns have been observed in mice based on LOAD genetics (R. S. Pandey et al., 2019; Preuss et al., 2020). In particular, we note that the neuroinflammatory responses in Consensus Cluster B driven by the GAB/CX3ert perturbation mimic those from APP/PS1 (Figure 6). The similar pattern of expression in the GAB/CX3ert x APP/PS1 double mutant suggests that the GAB/CX3ert mutation and APP/PS1 transgene are acting through similar mechanisms to generate this response; otherwise, we would have expected to see additive effects on each gene's expression. The overlap in GAB/CX3ert and APP/PS1 mice in NanoString targets coupled with the electrophysiological changes are particularly striking given the absence of any amyloid pathology in the GAB/CX3ert mice. This may point to an underlying molecular mechanism for the GAB/CX3ert mutation that mimics the response to transgenic amyloid, without any modifications of the standard gene targets *App*, *Psen1*, or *Psen2*. Together, these findings are particularly novel and may indicate that the some of the changes observed in amyloid mouse models may occur via loss of $GABA_B$ on glia. The alteration of $GABA_{B1}$ signaling on glia was capable of inducing amyloid related changes in the absence of amyloid.

To investigate how the reduction of the $GABA_BR$ and alterations in gene expression could influence AD pathology, we evaluated the Aβ in the non-amylogenic GAB/CX3ert mice crossbred with the APP/PS1 amyloid model (GAB/CX3ert x APP/PS1). Quantification of Aβ in male mice demonstrated that decreases in the $GABA_BR$ on macrophages results in a significant increase in Aβ-40 and Aβ-42 in GAB/CX3ert x APP/PS1 compared to APP/PS1 Aβ levels. In addition, gene expression data showed GAB/CX3ert x APP/PS1 mice had significantly increased expression of the *App* gene, when compared to the APP/PS1 alone, indicating a more pronounced effect. As described above, this may be a contributing factor to the greater amount of Aβ-40 and Aβ-42 in the GAB/CX3ert x APP/PS1 model compared to the APP/PS1 alone. A recent study by Rice et al. (2019) reported soluble APP, a precursor to the Aβ peptide, binds to the sushi domains of $GABA_B$, however, the authors explained the effects in neuronal processes. This interaction could be involved in the recognition of Aβ for phagocytosis and degradation of Aβ in glia cells. In the GAB/CX3ert, decrease of the receptor related to these processes could further explain the increase in Aβ. Furthermore, the increased expression of the *App* gene in the GAB/CX3ert x APP/PS1 may also be leading to the increase in Aβ production, in which the mechanisms for clearance fall further behind in processing the amyloid, however, this merits further investigation. The $GABA_BR$ was found to be significantly decreased in the APP/PS1 model at 6 months of age, indicating that the increased presence of Aβ leads to a loss of the protein (A. M. Salazar et al., 2021). Together, these data indicate a link between Aβ and $GABA_BR$, with previously reported findings of Aβ leading to decreases in $GABA_BR$ in APP/PS1 mice, and the reduction of the receptors exacerbating Aβ pathology in the current study. While our GAB/CX3ert x APP/PS1 mice

only carry one copy of the CX3CR1 after cross-breeding, genetic recombination possibly resulting in less GABA-BR knockdown than mice with both copies, still has a significant effect on Aβ levels, as future studies will aim to investigate the changes in Aβ in relation to the extent of GABA-BR knockdown.

It is interesting to note that the female GAB/CX3ert mice did not exhibit the same degree of loss of $GABA_BR$ as the males, and in fact it appears to be widely variable on an animal-to-animal basis in both the WT controls and GAB/CX3ert. With the genetic mutation being a creER model, which is activated through estrogen receptors, female and male mice may have different levels of genetic recombination (Donocoff et al., 2020; Kellendonk et al., 1999; Shimshek et al., 2002). Sex specific differences in recombination has been well described in mice (Rice, 2002; Ritz et al., 2017; Sardell & Kirkpatrick, 2020), as well as sex differences in both fAD and sAD mouse models (Li et al., 2016; Mishra et al., 2021; Oblak et al., 2021; Sun et al., 2020). While there were no significant differences in $GABA_BR$ levels in the overall female group, some females did show a loss. In addition, we do not report any significant changes in Aβ in the female GAB/CX3ert x APP/PS1 mice, as we observed in the males, which may be due to the inconstant $GABA_B$ reduction. The consistency in lack of altered $GABA_B$ and no change in amyloid in females further reinforces our data in the males. Changes in hormonal levels through the estrous cycle may be a contributing factor to $GABA_B$ expression and/or level of genetic recombination. Research has demonstrated that $GABA_B$ receptors may be regulated by sex hormones. In a study by Francois-Bellan et al., the authors demonstrated that chronic estradiol treatment resulted in a decrease in the density of $GABA_BR$ (François-Bellan et al., 1989). In addition, $GABA_B$ binding of baclofen, a $GABA_B$ agonist, was reported to vary throughout the estrous cycle, with highest binding during proestrus and lowest during the estrus stages (al-Dahan & Thalmann, 1996). The estrous cycle in our model may lead to the variability between the samples in female mice, depending on where the mice are in the cycle, resulting in no significant findings. Further evaluation of the GAB/CX3ert female mice and the $GABA_B$ receptor throughout the estrous cycle is required.

Our data demonstrate significant alterations in electrophysiological activity and gene expression in the non-amylogenic GAB/CX3ert mouse model, consistent with what is observed in a well-established amyloid model of AD. These findings indicate a novel mechanism, specifically the reduction in $GABA_B$ on glia induces similar alterations as a core pathology in AD. In addition, significant increases in Aβ were observed due to reductions in $GABA_BR$ on macrophages indicating a role for this receptor in amyloid production or clearance. Our findings provide support for further investigation of the role of $GABA_B$ on glia as a mechanism in AD pathogenesis.

Conclusion:

The GAB/CX3ert mouse model data provide several important novel implications in neurodegeneration disease research, particularly in the investigation of the $GABA_BR$'s role on glia function and AD. The reduction of $GABA_B$ on glia induced alterations in neuronal activity (sharp waves) and gene expression consistent with what is observed in amyloid fAD models is unique. This is particularly striking given there is no overt AD pathology

in these mice (Aβ or tau changes) and yet they exhibit several changes consistent with AD. These data suggest the alteration of $GABA_B$ on glia may be a mechanism in AD pathogenesis, potentially as a result of Aβ. In addition, we observed significant increases in Aβ-40 and Aβ-42 when our novel model was crossed with the APP/PS1 amyloid mouse model. These findings are particularly relevant as previous work has demonstrated in the APP/PS1 model a reduction of mRNA and total protein of $GABA_B$ (A. M. Salazar et al., 2021), which combined with the present study that reduced $GABA_B$ on glia exacerbates amyloid pathology, suggests a progressive relationship between amyloid and $GABA_B$. If amyloid induces a reduction of $GABA_B$, and that reduction exacerbates amyloid levels, our findings may provide a novel link between glia function and progressive amyloid accumulation. Further, the numerous gene expression targets altered in the GAB/CX3ert mouse model, that exhibits no amyloid pathology, indicates a conserved pathway in AD pathology. The GAB/CX3ert mice may serve as a novel model of AD without reliance on fAD genetic mutations, allowing further research into mechanisms of the disease, and possible therapeutic treatments.

Supplementary Material

Refer to Web version on PubMed Central for supplementary material.

Acknowledgements

The results published here are in whole or in part based on data obtained from the AD Knowledge Portal (https://adknowledgeportal.org). Study data were provided by the Rush Alzheimer's Disease Center, Rush University Medical Center, Chicago. Data collection was supported through funding by NIA grants P30AG10161 (ROS), R01AG15819 (ROSMAP; genomics and RNAseq), R01AG17917 (MAP), R01AG36836 (RNAseq), the Illinois Department of Public Health (ROSMAP), and the Translational Genomics Research Institute (genomic). Additional phenotypic data can be requested at www.radc.rush.edu. Mount Sinai Brain Bank data were generated from postmortem brain tissue collected through the Mount Sinai VA Medical Center Brain Bank and were provided by Dr. Eric Schadt from Mount Sinai School of Medicine. The Mayo RNAseq study data was led by Dr. Nilüfer Ertekin-Taner, Mayo Clinic, Jacksonville, FL as part of the multi-PI U01 AG046139 (MPIs Golde, Ertekin-Taner, Younkin, Price). Samples were provided from the following sources: The Mayo Clinic Brain Bank. Data collection was supported through funding by NIA grants P50 AG016574, R01 AG032990, U01 AG046139, R01 AG018023, U01 AG006576, U01 AG006786, R01 AG025711, R01 AG017216, R01 AG003949, NINDS grant R01 NS080820, CurePSP Foundation, and support from Mayo Foundation. Study data includes samples collected through the Sun Health Research Institute Brain and Body Donation Program of Sun City, Arizona. The Brain and Body Donation Program is supported by the National Institute of Neurological Disorders and Stroke (U24 NS072026 National Brain and Tissue Resource for Parkinsons Disease and Related Disorders), the National Institute on Aging (P30 AG19610 Arizona Alzheimers Disease Core Center), the Arizona Department of Health Services (contract 211002, Arizona Alzheimers Research Center), the Arizona Biomedical Research Commission (contracts 4001, 0011, 05–901 and 1001 to the Arizona Parkinson's Disease Consortium) and the Michael J. Fox Foundation for Parkinsons Research.

Funding Source:

NIGMS P20 COBRE Award (5P206M109025), NIA U54 054345 (G.W.C)

References:

2021 Alzheimer's disease facts and figures. (2021). Alzheimer's & Dementia: The Journal of the Alzheimer's Association, 17(3), 327–406. 10.1002/alz.12328

Agalave NM, Lane BT, Mody PH, Szabo-Pardi TA, & Burton MD (2020). Isolation, culture, and downstream characterization of primary microglia and astrocytes from adult rodent brain and spinal cord. Journal of Neuroscience Methods, 340, 108742. 10.1016/j.jneumeth.2020.108742

al-Dahan MI, & Thalmann RH (1996). Progesterone regulates gamma-aminobutyric acid B (GABAB) receptors in the neocortex of female rats. Brain Research, 727(1–2), 40–48.

Alam Q, Alam MZ, Mushtaq G, Damanhouri GA, Rasool M, Kamal MA, & Haque A (2016). Inflammatory Process in Alzheimer's and Parkinson's Diseases: Central Role of Cytokines. Current Pharmaceutical Design, 22(5), 541–548.

Álvarez-Aznar A, Martínez-Corral I, Daubel N, Betsholtz C, Mäkinen T, & Gaengel K (2020). Tamoxifen-independent recombination of reporter genes limits lineage tracing and mosaic analysis using CreERT2 lines. Transgenic Research, 29(1), 53–68. 10.1007/s11248-019-00177-8

Angelopoulou E, Paudel YN, Shaikh Mohd. F., & Piperi C (2020). Fractalkine (CX3CL1) signaling and neuroinflammation in Parkinson's disease: Potential clinical and therapeutic implications. Pharmacological Research, 158, 104930. 10.1016/j.phrs.2020.104930

Ardestani PM, Evans AK, Yi B, Nguyen T, Coutellier L, & Shamloo M (2017). Modulation of neuroinflammation and pathology in the 5XFAD mouse model of Alzheimer's disease using a biased and selective beta-1 adrenergic receptor partial agonist. Neuropharmacology, 116, 371–386. 10.1016/j.neuropharm.2017.01.010

Ballatore C, Lee VM-Y, & Trojanowski JQ (2007). Tau-mediated neurodegeneration in Alzheimer's disease and related disorders. Nature Reviews. Neuroscience, 8(9), 663–672. 10.1038/nrn2194

Bellucci A, Westwood AJ, Ingram E, Casamenti F, Goedert M, & Spillantini MG (2004). Induction of Inflammatory Mediators and Microglial Activation in Mice Transgenic for Mutant Human P301S Tau Protein. The American Journal of Pathology, 165(5), 1643–1652. 10.1016/S0002-9440(10)63421-9

Benarroch EE (2012). GABAB receptors. Neurology, 78(8), 578. 10.1212/WNL.0b013e318247cd03

Bettler B, Kaupmann K, Mosbacher J, & Gassmann M (2004). Molecular Structure and Physiological Functions of GABAB Receptors. Physiological Reviews, 84(3), 835–867. 10.1152/physrev.00036.2003

Biermann B, Ivankova-Susankova K, Bradaia A, Aziz SA, Besseyrias V, Kapfhammer JP, Missler M, Gassmann M, & Bettler B (2010). The Sushi Domains of GABAB Receptors Function as Axonal Targeting Signals. Journal of Neuroscience, 30(4), 1385–1394. 10.1523/JNEUROSCI.3172-09.2010

Blein S, Hawrot* E, & Barlow P (2000). The metabotropic GABA receptor: Molecular insights and their functional consequences. Cellular and Molecular Life Sciences CMLS, 57(4), 635–650. 10.1007/PL00000725

Bruttger J, Karram K, Wörtge S, Regen T, Marini F, Hoppmann N, Klein M, Blank T, Yona S, Wolf Y, Mack M, Pinteaux E, Müller W, Zipp F, Binder H, Bopp T, Prinz M, Jung S, & Waisman A (2015). Genetic Cell Ablation Reveals Clusters of Local Self-Renewing Microglia in the Mammalian Central Nervous System. Immunity, 43(1), 92–106. 10.1016/j.immuni.2015.06.012

Buzsáki G (1986). Hippocampal sharp waves: Their origin and significance. Brain Research, 398(2), 242–252. 10.1016/0006-8993(86)91483-6

Buzsáki G (2015). Hippocampal sharp wave-ripple: A cognitive biomarker for episodic memory and planning. Hippocampus, 25(10), 1073–1188. 10.1002/hipo.22488

Bygrave AM, Jahans-Price T, Wolff AR, Sprengel R, Kullmann DM, Bannerman DM, & Kätzel D (2019). Hippocampal–prefrontal coherence mediates working memory and selective attention at distinct frequency bands and provides a causal link between schizophrenia and its risk gene GRIA1. Translational Psychiatry, 9(1), Article 1. 10.1038/s41398-019-0471-0

Caccavano A, Bozzelli PL, Forcelli PA, Pak DTS, Wu J-Y, Conant K, & Vicini S (2020). Inhibitory Parvalbumin Basket Cell Activity is Selectively Reduced during Hippocampal Sharp Wave Ripples in a Mouse Model of Familial Alzheimer's Disease. Journal of Neuroscience, 40(26), 5116–5136. 10.1523/JNEUROSCI.0425-20.2020

Casanova E, Guetg N, Vigot R, Seddik R, Julio-Pieper M, Hyland NP, Cryan JF, Gassmann M, & Bettler B (2009). A mouse model for visualization of GABA(B) receptors. Genesis (New York, N.Y.: 2000), 47(9), 595–602. 10.1002/dvg.20535

Chappell-Maor L, Kolesnikov M, Kim J-S, Shemer A, Haimon Z, Grozovski J, Boura-Halfon S, Masuda T, Prinz M, & Jung S (2020). Comparative analysis of CreER transgenic mice for the

study of brain macrophages: A case study. European Journal of Immunology, 50(3), 353–362. 10.1002/eji.201948342

Charles KJ, Deuchars J, Davies CH, & Pangalos MN (2003). GABAB receptor subunit expression in glia. Molecular and Cellular Neuroscience, 24(1), 214–223. 10.1016/S1044-7431(03)00162-3

Crawley JN (1999). Behavioral phenotyping of transgenic and knockout mice: Experimental design and evaluation of general health, sensory functions, motor abilities, and specific behavioral tests. Brain Research, 835(1), 18–26. 10.1016/s0006-8993(98)01258-x

Crowley T, Fitzpatrick J-M, Kuijper T, Cryan JF, O'Toole O, O'Leary OF, & Downer EJ (2015). Modulation of TLR3/TLR4 inflammatory signaling by the GABAB receptor agonist baclofen in glia and immune cells: Relevance to therapeutic effects in multiple sclerosis. Frontiers in Cellular Neuroscience, 9. 10.3389/fncel.2015.00284

Davoodi FG, Motamedi F, Naghdi N, & Akbari E (2009). Effect of reversible inactivation of the reuniens nucleus on spatial learning and memory in rats using Morris water maze task. Behavioural Brain Research, 198(1), 130–135. 10.1016/j.bbr.2008.10.037

Donocoff RS, Teteloshvili N, Chung H, Shoulson R, & Creusot RJ (2020). Optimization of tamoxifen-induced Cre activity and its effect on immune cell populations. Scientific Reports, 10(1), Article 1. 10.1038/s41598-020-72179-0

Dubbelaar ML, Kracht L, Eggen BJL, & Boddeke EWGM (2018). The Kaleidoscope of Microglial Phenotypes. Frontiers in Immunology, 9. 10.3389/fimmu.2018.01753

Dumont M, Stack C, Elipenahli C, Jainuddin S, Gerges M, Starkova NN, Yang L, Starkov AA, & Beal F (2011). Behavioral deficit, oxidative stress, and mitochondrial dysfunction precede tau pathology in P301S transgenic mice. The FASEB Journal, 25(11), 4063–4072. 10.1096/fj.11-186650

Ego-Stengel V, & Wilson MA (2010). Disruption of ripple-associated hippocampal activity during rest impairs spatial learning in the rat. Hippocampus, 20(1), 1–10. 10.1002/hipo.20707

Favuzzi E, Huang S, Saldi GA, Binan L, Ibrahim LA, Fernández-Otero M, Cao Y, Zeine A, Sefah A, Zheng K, Xu Q, Khlestova E, Farhi SL, Bonneau R, Datta SR, Stevens B, & Fishell G (2021). GABA-receptive microglia selectively sculpt developing inhibitory circuits. Cell, 184(15), 4048–4063.e32. 10.1016/j.cell.2021.06.018

Fjell AM, McEvoy L, Holland D, Dale AM, Walhovd KB, & Alzheimer's Disease Neuroimaging Initiative. (2014). What is normal in normal aging? Effects of aging, amyloid and Alzheimer's disease on the cerebral cortex and the hippocampus. Progress in Neurobiology, 117, 20–40. 10.1016/j.pneurobio.2014.02.004

Fonseca MI, Chu S-H, Hernandez MX, Fang MJ, Modarresi L, Selvan P, MacGregor GR, & Tenner AJ (2017). Cell-specific deletion of C1qa identifies microglia as the dominant source of C1q in mouse brain. Journal of Neuroinflammation, 14. 10.1186/s12974-017-0814-9

François-Bellan AM, Segu L, & Héry M (1989). Regulation by estradiol of GABAA and GABAB binding sites in the diencephalon of the rat: An autoradiographic study. Brain Research, 503(1), 144–147. 10.1016/0006-8993(89)91715-0

Fries P (2015). Rhythms For Cognition: Communication Through Coherence. Neuron, 88(1), 220–235. 10.1016/j.neuron.2015.09.034

Gaiarsa J-L, Kuczewski N, & Porcher C (2011). Contribution of metabotropic GABAB receptors to neuronal network construction. Pharmacology & Therapeutics, 132(2), 170–179. 10.1016/j.pharmthera.2011.06.004

Gassmann M, & Bettler B (2012). Regulation of neuronal GABAB receptor functions by subunit composition. Nature Reviews Neuroscience, 13(6), 380–394. 10.1038/nrn3249

Giulian D, Li J, Li X, George J, & Rutecki PA (1994). The Impact of Microglia-Derived Cytokines upon Gliosis in the CNS. Developmental Neuroscience, 16(3–4), 128–136. 10.1159/000112099

Goldmann T, Wieghofer P, Müller PF, Wolf Y, Varol D, Yona S, Brendecke SM, Kierdorf K, Staszewski O, Datta M, Luedde T, Heikenwalder M, Jung S, & Prinz M (2013). A new type of microglia gene targeting shows TAK1 to be pivotal in CNS autoimmune inflammation. Nature Neuroscience, 16(11), 1618. 10.1038/nn.3531

González-Scarano F, & Baltuch G (1999). Microglia as Mediators of Inflammatory and Degenerative Diseases. Annual Review of Neuroscience, 22(1), 219–240. 10.1146/annurev.neuro.22.1.219

Guerreiro R, Wojtas A, Bras J, Carrasquillo M, Rogaeva E, Majounie E, Cruchaga C, Sassi C, Kauwe JSK, Younkin S, Hazrati L, Collinge J, Pocock J, Lashley T, Williams J, Lambert J-C, Amouyel P, Goate A, Rademakers R, … Hardy J (2013). TREM2 Variants in Alzheimer's Disease. The New England Journal of Medicine, 368(2), 117–127. 10.1056/NEJMoa1211851

Guetg N, Seddik R, Vigot R, Turecek R, Gassmann M, Vogt KE, Bräuner-Osborne H, Shigemoto R, Kretz O, Frotscher M, Kulik A, & Bettler B (2009). The GABAB1a isoform mediates heterosynaptic depression at hippocampal mossy fiber synapses. The Journal of Neuroscience: The Official Journal of the Society for Neuroscience, 29(5), 1414–1423. 10.1523/JNEUROSCI.3697-08.2009

Haller C, Casanova E, Müller M, Vacher C-M, Vigot R, Doll T, Barbieri S, Gassmann M, & Bettler B (2004). Floxed allele for conditional inactivation of the GABAB(1) gene. Genesis (New York, N.Y.: 2000), 40(3), 125–130. 10.1002/gene.20073

Hallock HL, Wang A, Shaw CL, & Griffin AL (2013). Transient inactivation of the thalamic nucleus reuniens and rhomboid nucleus produces deficits of a working-memory dependent tactile-visual conditional discrimination task. Behavioral Neuroscience, 127(6), 860–866. 10.1037/a0034653

Hammond TR, Marsh SE, & Stevens B (2019). Immune Signaling in Neurodegeneration. Immunity, 50(4), 955–974. 10.1016/j.immuni.2019.03.016

Hannan S, Wilkins ME, & Smart TG (2012). Sushi domains confer distinct trafficking profiles on GABAB receptors. Proceedings of the National Academy of Sciences, 109(30), 12171–12176. 10.1073/pnas.1201660109

Hanseeuw BJ, Betensky RA, Jacobs HIL, Schultz AP, Sepulcre J, Becker JA, Cosio DMO, Farrell M, Quiroz YT, Mormino EC, Buckley RF, Papp KV, Amariglio RA, Dewachter I, Ivanoiu A, Huijbers W, Hedden T, Marshall GA, Chhatwal JP, … Johnson K (2019). Association of Amyloid and Tau With Cognition in Preclinical Alzheimer Disease: A Longitudinal Study. JAMA Neurology, 76(8), 915–924. 10.1001/jamaneurol.2019.1424

Haque ME, Kim I-S, Jakaria M, Akther M, & Choi D-K (2018). Importance of GPCR-Mediated Microglial Activation in Alzheimer's Disease. Frontiers in Cellular Neuroscience, 12. 10.3389/fncel.2018.00258

Edward Hawrot, Yuanyuan Xiao, Qing-luo Shi, David Norman, Marina Kirkitadze, & Barlow Paul N. (1998). Demonstration of a tandem pair of complement protein modules in GABAB receptor 1a. FEBS Letters, 432(3), 103–108. 10.1016/S0014-5793(98)00794-7

Heaney CF, & Kinney JW (2016). Role of GABAB receptors in learning and memory and neurological disorders. Neuroscience & Biobehavioral Reviews, 63, 1–28. 10.1016/j.neubiorev.2016.01.007

Hickman SE, Allison EK, & Khoury JE (2008). Microglial dysfunction and defective β-amyloid clearance pathways in aging Alzheimer's disease mice. The Journal of Neuroscience : The Official Journal of the Society for Neuroscience, 28(33), 8354–8360. 10.1523/JNEUROSCI.0616-08.2008

Hickman S, Izzy S, Sen P, Morsett L, & El Khoury J (2018). Microglia in neurodegeneration. Nature Neuroscience, 21(10), Article 10. 10.1038/s41593-018-0242-x

Hu Y, Fryatt GL, Ghorbani M, Obst J, Menassa DA, Martin-Estebane M, Muntslag TAO, Olmos-Alonso A, Guerrero-Carrasco M, Thomas D, Cragg MS, & Gomez-Nicola D (2021). Replicative senescence dictates the emergence of disease-associated microglia and contributes to Aβ pathology. Cell Reports, 35(10), 109228. 10.1016/j.celrep.2021.109228

Hurst JL, & West RS (2010). Taming anxiety in laboratory mice. Nature Methods, 7(10), Article 10. 10.1038/nmeth.1500

Ishibashi M, Egawa K, & Fukuda A (2019). Diverse Actions of Astrocytes in GABAergic Signaling. International Journal of Molecular Sciences, 20(12). 10.3390/ijms20122964

Jay TR, Hirsch AM, Broihier ML, Miller CM, Neilson LE, Ransohoff RM, Lamb BT, & Landreth GE (2017). Disease Progression-Dependent Effects of TREM2 Deficiency in a Mouse Model of Alzheimer's Disease. The Journal of Neuroscience, 37(3), 637–647. 10.1523/JNEUROSCI.2110-16.2016

Jiang T, Zhang Y-D, Chen Q, Gao Q, Zhu X-C, Zhou J-S, Shi J-Q, Lu H, Tan L, & Yu J-T (2016). TREM2 modifies microglial phenotype and provides neuroprotection in P301S tau transgenic mice. Neuropharmacology, 105, 196–206. 10.1016/j.neuropharm.2016.01.028

Jo S, Yarishkin O, Hwang YJ, Chun YE, Park M, Woo DH, Bae JY, Kim T, Lee J, Chun H, Park HJ, Lee DY, Hong J, Kim HY, Oh S-J, Park SJ, Lee H, Yoon B-E, Kim Y, … Lee CJ (2014). GABA from reactive astrocytes impairs memory in mouse models of Alzheimer's disease. Nature Medicine, 20(8), 886. 10.1038/nm.3639

Jones EA, Gillespie AK, Yoon SY, Frank LM, & Huang Y (2019). Early Hippocampal Sharp-Wave Ripple Deficits Predict Later Learning and Memory Impairments in an Alzheimer's Disease Mouse Model. Cell Reports, 29(8), 2123–2133.e4. 10.1016/j.celrep.2019.10.056

Jones MW, & Wilson MA (2005). Theta Rhythms Coordinate Hippocampal–Prefrontal Interactions in a Spatial Memory Task. PLOS Biology, 3(12), e402. 10.1371/journal.pbio.0030402

Joo HR, & Frank LM (2018). The hippocampal sharp wave-ripple in memory retrieval for immediate use and consolidation. Nature Reviews. Neuroscience, 19(12), 744–757. 10.1038/s41583-018-0077-1

Jura B, Macrez N, Meyrand P, & Bem T (2019). Deficit in hippocampal ripples does not preclude spatial memory formation in APP/PS1 mice. Scientific Reports, 9(1), Article 1. 10.1038/s41598-019-56582-w

Kantamneni S (2015). Cross-talk and regulation between glutamate and GABAB receptors. Frontiers in Cellular Neuroscience, 9. 10.3389/fncel.2015.00135

Kay K, Sosa M, Chung JE, Karlsson MP, Larkin MC, & Frank LM (2016). A hippocampal network for spatial coding during immobility and sleep. Nature, 531(7593), Article 7593. 10.1038/nature17144

Kellendonk C, Tronche F, Casanova E, Anlag K, Opherk C, & Schütz G (1999). Inducible site-specific recombination in the brain11Edited by M. Yaniv. Journal of Molecular Biology, 285(1), 175–182. 10.1006/jmbi.1998.2307

King JR, Gillevet TC, & Kabbani N (2017). A G protein-coupled α7 nicotinic receptor regulates signaling and TNF-α release in microglia. FEBS Open Bio, 7(9), 1350–1361. 10.1002/2211-5463.12270

Kinney JW, Bemiller SM, Murtishaw AS, Leisgang AM, Salazar AM, & Lamb BT (2018). Inflammation as a central mechanism in Alzheimer's disease. Alzheimer's & Dementia : Translational Research & Clinical Interventions, 4, 575–590. 10.1016/j.trci.2018.06.014

Kohl MM, & Paulsen O (2010). The Roles of GABAB Receptors in Cortical Network Activity. In Blackburn TP (Ed.), Advances in Pharmacology (Vol. 58, pp. 205–229). Academic Press. 10.1016/S1054-3589(10)58009-8

Koller EJ, De La Cruz EG, Weinrich MJ, Antezana G, Ibanez KR, Ryu DH, Lewis J, & Chakrabarty P (2020). Effect of soluble interleukin-10 receptor expression in mouse models of Alzheimer's disease. Alzheimer's & Dementia, 16(S2), e041927. 10.1002/alz.041927

Krabbe G, Halle A, Matyash V, Rinnenthal JL, Eom GD, Bernhardt U, Miller KR, Prokop S, Kettenmann H, & Heppner FL (2013). Functional Impairment of Microglia Coincides with Beta-Amyloid Deposition in Mice with Alzheimer-Like Pathology. PLOS ONE, 8(4), e60921. 10.1371/journal.pone.0060921

Kristianto J, Johnson MG, Zastrow RK, Radcliff AB, & Blank RD (2017). Spontaneous recombinase activity of Cre–ERT2 in vivo. Transgenic Research, 26(3), 411–417. 10.1007/s11248-017-0018-1

Kuhn SA, van Landeghem FKH, Zacharias R, Färber K, Rappert A, Pavlovic S, Hoffmann A, Nolte C, & Kettenmann H (2004). Microglia express GABA B receptors to modulate interleukin release. Molecular and Cellular Neuroscience, 25(2), 312–322. 10.1016/j.mcn.2003.10.023

La Joie R, Visani AV, Baker SL, Brown JA, Bourakova V, Cha J, Chaudhary K, Edwards L, Iaccarino L, Janabi M, Lesman-Segev OH, Miller ZA, Perry DC, O'Neil JP, Pham J, Rojas JC, Rosen HJ, Seeley WW, Tsai RM, … Rabinovici GD (2020). Prospective longitudinal atrophy in Alzheimer's disease correlates with the intensity and topography of baseline tau-PET. Science Translational Medicine, 12(524), eaau5732. 10.1126/scitranslmed.aau5732

Le Meur K, Mendizabal-Zubiaga J, Grandes P, & Audinat E (2012). GABA release by hippocampal astrocytes. Frontiers in Computational Neuroscience, 6. 10.3389/fncom.2012.00059

Lee JY, Jhun BS, Oh YT, Lee JH, Choe W, Baik HH, Ha J, Yoon K-S, Kim SS, & Kang I (2006). Activation of adenosine A3 receptor suppresses lipopolysaccharide-induced TNF-alpha production through inhibition of PI 3-kinase/Akt and NF-kappaB activation in murine BV2 microglial cells. Neuroscience Letters, 396(1), 1–6. 10.1016/j.neulet.2005.11.004

Lee M, McGeer EG, & McGeer PL (2011). Mechanisms of GABA release from human astrocytes. Glia, 59(11), 1600–1611. 10.1002/glia.21202

Lee M, Schwab C, & Mcgeer PL (2011). Astrocytes are GABAergic cells that modulate microglial activity. Glia, 59(1), 152–165. 10.1002/glia.21087

Li M, Long C, & Yang L (2015). Hippocampal-prefrontal circuit and disrupted functional connectivity in psychiatric and neurodegenerative disorders. BioMed Research International, 2015, 810548. 10.1155/2015/810548

Li X, Du Z-J, Chen M-Q, Chen J-J, Liang Z-M, Ding X-T, Zhou M, Li S-J, Li X-W, Yang J-M, & Gao T-M (2020). The effects of tamoxifen on mouse behavior. Genes, Brain and Behavior, 19(4), e12620. 10.1111/gbb.12620

Li X, Feng Y, Wu W, Zhao J, Fu C, Li Y, Ding Y, Wu B, Gong Y, Yang G, & Zhou X (2016). Sex differences between APPswePS1dE9 mice in A-beta accumulation and pancreatic islet function during the development of Alzheimer's disease. Laboratory Animals, 50(4), 275–285. 10.1177/0023677215615269

Li Y, Sun H, Chen Z, Xu H, Bu G, & Zheng H (2016). Implications of GABAergic Neurotransmission in Alzheimer's Disease. Frontiers in Aging Neuroscience, 8. 10.3389/fnagi.2016.00031

Liu B, & Hong J-S (2003). Role of Microglia in Inflammation-Mediated Neurodegenerative Diseases: Mechanisms and Strategies for Therapeutic Intervention. Journal of Pharmacology and Experimental Therapeutics, 304(1), 1–7. 10.1124/jpet.102.035048

Liu Z, Qiu A-W, Huang Y, Yang Y, Chen J-N, Gu T-T, Cao B-B, Qiu Y-H, & Peng Y-P (2019). IL-17A exacerbates neuroinflammation and neurodegeneration by activating microglia in rodent models of Parkinson's disease. Brain, Behavior, and Immunity, 81, 630–645. 10.1016/j.bbi.2019.07.026

Lok K, Zhao H, Shen H, Wang Z, Gao X, Zhao W, & Yin M (2013). Characterization of the APP/PS1 mouse model of Alzheimer's disease in senescence accelerated background. Neuroscience Letters, 557 Pt B, 84–89. 10.1016/j.neulet.2013.10.051

Lopes G, Bonacchi N, Frazão J, Neto JP, Atallah BV, Soares S, Moreira L, Matias S, Itskov PM, Correia PA, Medina RE, Calcaterra L, Dreosti E, Paton JJ, & Kampff AR (2015). Bonsai: An event-based framework for processing and controlling data streams. Frontiers in Neuroinformatics, 9. 10.3389/fninf.2015.00007

Lull ME, & Block ML (2010). Microglial Activation and Chronic Neurodegeneration. Neurotherapeutics, 7(4), 354–365. 10.1016/j.nurt.2010.05.014

Makino Y, Polygalov D, Bolaños F, Benucci A, & McHugh TJ (2019). Physiological Signature of Memory Age in the Prefrontal-Hippocampal Circuit. Cell Reports, 29(12), 3835–3846.e5. 10.1016/j.celrep.2019.11.075

Mandelkow E-M, & Mandelkow E (1998). Tau in Alzheimer's disease. Trends in Cell Biology, 8(11), 425–427. 10.1016/S0962-8924(98)01368-3

Mandrekar S, & Landreth GE (2010). Microglia and Inflammation in Alzheimer's Disease. CNS & Neurological Disorders Drug Targets, 9(2), 156–167.

Marshall FH, Jones KA, Kaupmann K, & Bettler B (1999). GABAB receptors – the first 7TM heterodimers. Trends in Pharmacological Sciences, 20(10), 396–399. 10.1016/S0165-6147(99)01383-8

McQuade A, Kang YJ, Hasselmann J, Jairaman A, Sotelo A, Coburn M, Shabestari SK, Chadarevian JP, Fote G, Tu CH, Danhash E, Silva J, Martinez E, Cotman C, Prieto GA, Thompson LM, Steffan JS, Smith I, Davtyan H, … Blurton-Jones M (2020). Gene expression and functional deficits underlie TREM2-knockout microglia responses in human models of Alzheimer's disease. Nature Communications, 11(1), Article 1. 10.1038/s41467-020-19227-5

Meda L, Cassatella MA, Szendrei GI, Otvos L, Baron P, Villalba M, Ferrari D, & Rossi F (1995). Activation of microglial cells by beta-amyloid protein and interferon-gamma. Nature, 374(6523), 647–650. 10.1038/374647a0

Medeiros R, Baglietto-Vargas D, & LaFerla FM (2010). The Role of Tau in Alzheimer's Disease and Related Disorders. CNS Neuroscience & Therapeutics, 17(5), 514–524. 10.1111/j.1755-5949.2010.00177.x

Mishra A, Soto M, Delatorre N, Rodgers KE, & Brinton RD (2021). APOE4 genetic burden and female sex impact immune profile in brain and periphery in aged mice. Alzheimer's & Dementia, 17(S3), e056541. 10.1002/alz.056541

Müller UC, Deller T, & Korte M (2017). Not just amyloid: Physiological functions of the amyloid precursor protein family. Nature Reviews Neuroscience, 18(5), 281–298. 10.1038/nrn.2017.29

Murtishaw AS, Heaney CF, Bolton MM, Belmonte KCD, Langhardt MA, & Kinney JW (2018). Intermittent streptozotocin administration induces behavioral and pathological features relevant to Alzheimer's disease and vascular dementia. Neuropharmacology, 137, 164–177. 10.1016/j.neuropharm.2018.04.021

Nava Catorce M, Acero G, & Gevorkian G (2021). Age- and sex-dependent alterations in the peripheral immune system in the 3xTg-AD mouse model of Alzheimer's disease: Increased proportion of CD3+CD4-CD8- double-negative T cells in the blood. Journal of Neuroimmunology, 360, 577720. 10.1016/j.jneuroim.2021.577720

Navarro V, Sanchez-Mejias E, Jimenez S, Muñoz-Castro C, Sanchez-Varo R, Davila JC, Vizuete M, Gutierrez A, & Vitorica J (2018). Microglia in Alzheimer's Disease: Activated, Dysfunctional or Degenerative. Frontiers in Aging Neuroscience, 10. 10.3389/fnagi.2018.00140

Oblak AL, Lin PB, Kotredes KP, Pandey RS, Garceau D, Williams HM, Uyar A, O'Rourke R, O'Rourke S, Ingraham C, Bednarczyk D, Belanger M, Cope ZA, Little GJ, Williams S-PG, Ash C, Bleckert A, Ragan T, Logsdon BA, … Lamb BT (2021). Comprehensive Evaluation of the 5XFAD Mouse Model for Preclinical Testing Applications: A MODEL-AD Study. Frontiers in Aging Neuroscience, 13, 713726. 10.3389/fnagi.2021.713726

Pandey D, Banerjee S, Basu M, & Mishra N (2016). Memory enhancement by Tamoxifen on amyloidosis mouse model. Hormones and Behavior, 79, 70–73. 10.1016/j.yhbeh.2015.09.004

Pandey RS, Graham L, Uyar A, Preuss C, Howell GR, & Carter GW (2019). Genetic perturbations of disease risk genes in mice capture transcriptomic signatures of late-onset Alzheimer's disease. Molecular Neurodegeneration, 14(1), 50. 10.1186/s13024-019-0351-3

Parkhurst CN, Yang G, Ninan I, Savas JN, Yates JR, Lafaille JJ, Hempstead BL, Littman DR, & Gan W-B (2013). Microglia promote learning-dependent synapse formation through BDNF. Cell, 155(7), 1596–1609. 10.1016/j.cell.2013.11.030

Perea JR, Llorens-Martín M, Ávila J, & Bolós M (2018). The Role of Microglia in the Spread of Tau: Relevance for Tauopathies. Frontiers in Cellular Neuroscience, 12. 10.3389/fncel.2018.00172

Pfeiffer BE, & Foster DJ (2013). Hippocampal place-cell sequences depict future paths to remembered goals. Nature, 497(7447), Article 7447. 10.1038/nature12112

Pillon NJ, Smith JAB, Alm PS, Chibalin AV, Alhusen J, Arner E, Carninci P, Fritz T, Otten J, Olsson T, van Doorslaer de ten Ryen S, Deldicque L, Caidahl K, Wallberg-Henriksson H, Krook A, & Zierath JR (2022). Distinctive exercise-induced inflammatory response and exerkine induction in skeletal muscle of people with type 2 diabetes. Science Advances, 8(36), eabo3192. 10.1126/sciadv.abo3192

Preuss C, Pandey R, Piazza E, Fine A, Uyar A, Perumal T, Garceau D, Kotredes KP, Williams H, Mangravite LM, Lamb BT, Oblak AL, Howell GR, Sasner M, Logsdon BA, MODEL-AD Consortium, & Carter GW (2020). A novel systems biology approach to evaluate mouse models of late-onset Alzheimer's disease. Molecular Neurodegeneration, 15(1), 67. 10.1186/s13024-020-00412-5

Prosser HM, Gill CH, Hirst WD, Grau E, Robbins M, Calver A, Soffin EM, Farmer CE, Lanneau C, Gray J, Schenck E, Warmerdam BS, Clapham C, Reavill C, Rogers DC, Stean T, Upton N, Humphreys K, Randall A, … Pangalos MN (2001). Epileptogenesis and Enhanced Prepulse Inhibition in GABAB1-Deficient Mice. Molecular and Cellular Neuroscience, 17(6), 1059–1070. 10.1006/mcne.2001.0995

Quéva C, Bremner-Danielsen M, Edlund A, Jonas Ekstrand A, Elg S, Erickson S, Johansson T, Lehmann A, & Mattsson JP (2003). Effects of GABA agonists on body temperature regulation in GABAB(1)−/− mice. British Journal of Pharmacology, 140(2), 315–322. 10.1038/sj.bjp.0705447

Ramanathan KR, Ressler RL, Jin J, & Maren S (2018). Nucleus Reuniens Is Required for Encoding and Retrieving Precise, Hippocampal-Dependent Contextual Fear Memories in Rats. The Journal of Neuroscience: The Official Journal of the Society for Neuroscience, 38(46), 9925–9933. 10.1523/JNEUROSCI.1429-18.2018

Ranasinghe KG, Petersen C, Kudo K, Srivatsan S, Beagle AJ, Mizuiri D, Findlay A, Houde JF, Rankin K, Rabinovici GD, Seeley WW, Spina S, Gorno-Tempini M, Kramer JH, Miller BL, Vossel KA, Grinberg LT, & Nagarajan SS (2020). Alpha-frequency synchronization deficits during life predict postmortem neurofibrillary tangle burden in Alzheimer's disease. Alzheimer's & Dementia, 16(S4), e045351. 10.1002/alz.045351

Rice HC, de Malmazet D, Schreurs A, Frere S, Van Molle I, Volkov AN, Creemers E, Vertkin I, Nys J, Ranaivoson FM, Comoletti D, Savas JN, Remaut H, Balschun D, Wierda KD, Slutsky I, Farrow K, De Strooper B, & de Wit J (2019). Secreted Amyloid-β Precursor Protein Functions as a GABABR1a Ligand to Modulate Synaptic Transmission. Science (New York, N.Y.), 363(6423). 10.1126/science.aao4827

Rice WR (2002). Experimental tests of the adaptive significance of sexual recombination. Nature Reviews Genetics, 3(4), Article 4. 10.1038/nrg760

Ritz KR, Noor MAF, & Singh ND (2017). Variation in Recombination Rate: Adaptive or Not? Trends in Genetics, 33(5), 364–374. 10.1016/j.tig.2017.03.003

Sahasrabuddhe V, & Ghosh HS (2022). Cx3Cr1-Cre induction leads to microglial activation and IFN-1 signaling caused by DNA damage in early postnatal brain. Cell Reports, 38(3), 110252. 10.1016/j.celrep.2021.110252

Salazar A, Leisgang A, Ortiz A, & Kinney J (2019). Dementia Insights: What Do Animal Models of Alzheimer's Disease Tell Us? Practical Neurology.

Salazar AM, Leisgang AM, Ortiz AA, Murtishaw AS, & Kinney JW (2021). Alterations of GABA B receptors in the APP/PS1 mouse model of Alzheimer's disease. Neurobiology of Aging, 97, 129–143. 10.1016/j.neurobiolaging.2020.10.013

Sardell JM, & Kirkpatrick M (2020). Sex differences in the recombination landscape. The American Naturalist, 195(2), 361–379. 10.1086/704943

Sawada M, Imamura K, & Nagatsu T (2006). Role of cytokines in inflammatory process in Parkinson's disease. Journal of Neural Transmission. Supplementum, 70, 373–381. 10.1007/978-3-211-45295-0_57

Schultheiss NW, Schlecht M, Jayachandran M, Brooks DR, McGlothan JL, Guilarte TR, & Allen TA (2020). Awake delta and theta-rhythmic hippocampal network modes during intermittent locomotor behaviors in the rat. Behavioral Neuroscience, 134(6), 529–546. 10.1037/bne0000409

Shen W, Nan C, Nelson PT, Ripps H, & Slaughter MM (2017). GABAB receptor attenuation of GABAA currents in neurons of the mammalian central nervous system. Physiological Reports, 5(6). 10.14814/phy2.13129

Sheng JG, Zhou XQ, Mrak RE, & Griffin WST (1998). Progressive Neuronal Injury Associated with Amyloid Plaque Formation in Alzheimer Disease. Journal of Neuropathology & Experimental Neurology, 57(7), 714–717. 10.1097/00005072-199807000-00008

Shimshek D. r., Kim J, Hübner M. r., Spergel D. j., Buchholz F, Casanova E, Stewart A. f., Seeburg P. h., & Sprengel R (2002). Codon-improved Cre recombinase (iCre) expression in the mouse. Genesis, 32(1), 19–26. 10.1002/gene.10023

Sigurdsson T, Stark KL, Karayiorgou M, Gogos JA, & Gordon JA (2010). Impaired hippocampal–prefrontal synchrony in a genetic mouse model of schizophrenia. Nature, 464(7289), Article 7289. 10.1038/nature08855

Smith JA, Das A, Ray SK, & Banik NL (2012). Role of pro-inflammatory cytokines released from microglia in neurodegenerative diseases. Brain Research Bulletin, 87(1), 10–20. 10.1016/j.brainresbull.2011.10.004

Španić E, Langer Horvat L, Hof PR, & Šimić G (2019). Role of Microglial Cells in Alzheimer's Disease Tau Propagation. Frontiers in Aging Neuroscience, 11. 10.3389/fnagi.2019.00271

Streit WJ, Walter SA, & Pennell NA (1999). Reactive microgliosis. Progress in Neurobiology, 57(6), 563–581. 10.1016/S0301-0082(98)00069-0

Subramanian A, Tamayo P, Mootha VK, Mukherjee S, Ebert BL, Gillette MA, Paulovich A, Pomeroy SL, Golub TR, Lander ES, & Mesirov JP (2005). Gene set enrichment analysis: A knowledge-based approach for interpreting genome-wide expression profiles. Proceedings of the National Academy of Sciences, 102(43), 15545–15550. 10.1073/pnas.0506580102

Sun Y, Guo Y, Feng X, Jia M, Ai N, Dong Y, Zheng Y, Fu L, Yu B, Zhang H, Wu J, Yu X, Wu H, & Kong W (2020). The behavioural and neuropathologic sexual dimorphism and absence of MIP-3α in tau P301S mouse model of Alzheimer's disease. Journal of Neuroinflammation, 17(1), 72. 10.1186/s12974-020-01749-w

Talan J (2019). Depleting Microglia Prevents Amyloid-Beta Plaque Formation. Neurology Today, 19(19), 30. 10.1097/01.NT.0000602968.05625.3a

Tang W, & Jadhav SP (2019). Sharp-wave ripples as a signature of hippocampal-prefrontal reactivation for memory during sleep and waking states. Neurobiology of Learning and Memory, 160, 11–20. 10.1016/j.nlm.2018.01.002

Tay TL, Mai D, Dautzenberg J, Fernández-Klett F, Lin G, Sagar, Datta M, Drougard A, Stempfl T, Ardura-Fabregat A, Staszewski O, Margineanu A, Sporbert A, Steinmetz LM, Pospisilik JA, Jung S, Priller J, Grün D, Ronneberger O, & Prinz M (2017). A new fate mapping system reveals context-dependent random or clonal expansion of microglia. Nature Neuroscience, 20(6), Article 6. 10.1038/nn.4547

Tremblay M-È, Stevens B, Sierra A, Wake H, Bessis A, & Nimmerjahn A (2011). The Role of Microglia in the Healthy Brain. Journal of Neuroscience, 31(45), 16064–16069. 10.1523/JNEUROSCI.4158-11.2011

Van Hove H, Antunes ARP, De Vlaminck K, Scheyltjens I, Van Ginderachter JA, & Movahedi K (2020). Identifying the variables that drive tamoxifen-independent CreERT2 recombination: Implications for microglial fate mapping and gene deletions. European Journal of Immunology, 50(3), 459–463. 10.1002/eji.201948162

Wan Y-W, Al-Ouran R, Mangleburg CG, Perumal TM, Lee TV, Allison K, Swarup V, Funk CC, Gaiteri C, Allen M, Wang M, Neuner SM, Kaczorowski CC, Philip VM, Howell GR, Martini-Stoica H, Zheng H, Mei H, Zhong X, … Logsdon BA (2020). Meta-Analysis of the Alzheimer's Disease Human Brain Transcriptome and Functional Dissection in Mouse Models. Cell Reports, 32(2), 107908. 10.1016/j.celrep.2020.107908

Wang C-C, Wee H-Y, Chio C-C, Hu C-Y, & Kuo J-R (2016). Effects of tamoxifen on traumatic brain injury-induced depression in male rats. Formosan Journal of Surgery, 49(3), 101–109. 10.1016/j.fjs.2015.12.003

Wirt RA, Crew LA, Ortiz AA, McNeela AM, Flores E, Kinney JW, & Hyman JM (2021). Altered theta rhythm and hippocampal-cortical interactions underlie working memory deficits in a hyperglycemia risk factor model of Alzheimer's disease. Communications Biology, 4(1), Article 1. 10.1038/s42003-021-02558-4

Wirt RA, & Hyman JM (2019). ACC Theta Improves Hippocampal Contextual Processing during Remote Recall. Cell Reports, 27(8), 2313–2327.e4. 10.1016/j.celrep.2019.04.080

Wrenn CC, Kinney JW, Marriott LK, Holmes A, Harris AP, Saavedra MC, Starosta G, Innerfield CE, Jacoby AS, Shine J, Iismaa TP, Wenk GL, & Crawley JN (2004). Learning and memory performance in mice lacking the GAL-R1 subtype of galanin receptor. The European Journal of Neuroscience, 19(5), 1384–1396. 10.1111/j.1460-9568.2004.03214.x

Wu T, Hu E, Xu S, Chen M, Guo P, Dai Z, Feng T, Zhou L, Tang W, Zhan L, Fu X, Liu S, Bo X, & Yu G (2021). clusterProfiler 4.0: A universal enrichment tool for interpreting omics data. Innovation (Cambridge (Mass.)), 2(3), 100141. 10.1016/j.xinn.2021.100141

Xu L, He D, & Bai Y (2016). Microglia-Mediated Inflammation and Neurodegenerative Disease. Molecular Neurobiology, 53(10), 6709–6715. 10.1007/s12035-015-9593-4

Yang H-M, Yang S, Huang S-S, Tang B-S, & Guo J-F (2017). Microglial Activation in the Pathogenesis of Huntington's Disease. Frontiers in Aging Neuroscience, 9. 10.3389/fnagi.2017.00193

Yankner BA, & Lu T (2009). Amyloid β-Protein Toxicity and the Pathogenesis of Alzheimer Disease. The Journal of Biological Chemistry, 284(8), 4755–4759. 10.1074/jbc.R800018200

Zhao X-F, Alam MM, Liao Y, Huang T, Mathur R, Zhu X, & Huang Y (2019). Targeting Microglia Using Cx3cr1-Cre Lines: Revisiting the Specificity. ENeuro, 6(4). 10.1523/ENEURO.0114-19.2019

Zhurakovskaya E, Ishchenko I, Gureviciene I, Aliev R, Gröhn O, & Tanila H (2019). Impaired hippocampal-cortical coupling but preserved local synchrony during sleep in APP/PS1 mice modeling Alzheimer's disease. Scientific Reports, 9(1), Article 1. 10.1038/s41598-019-41851-5

Zielinski MC, Shin JD, & Jadhav SP (2019). Coherent Coding of Spatial Position Mediated by Theta Oscillations in the Hippocampus and Prefrontal Cortex. Journal of Neuroscience, 39(23), 4550–4565. 10.1523/JNEUROSCI.0106-19.2019

Highlights

- Decreasing $GABA_BR$ on macrophages in APP/PS1 mice results in increased in amyloid
- Network activity of GAB/CX3ert mice is comparable to the APP/PS1 model
- GAB/CX3ert mice express risk factor genes observed in APP/PS1 mice and human AD
- GAB/CX3ert show consistencies with APP/PS1 mice, unique to non-amyloidogenic models

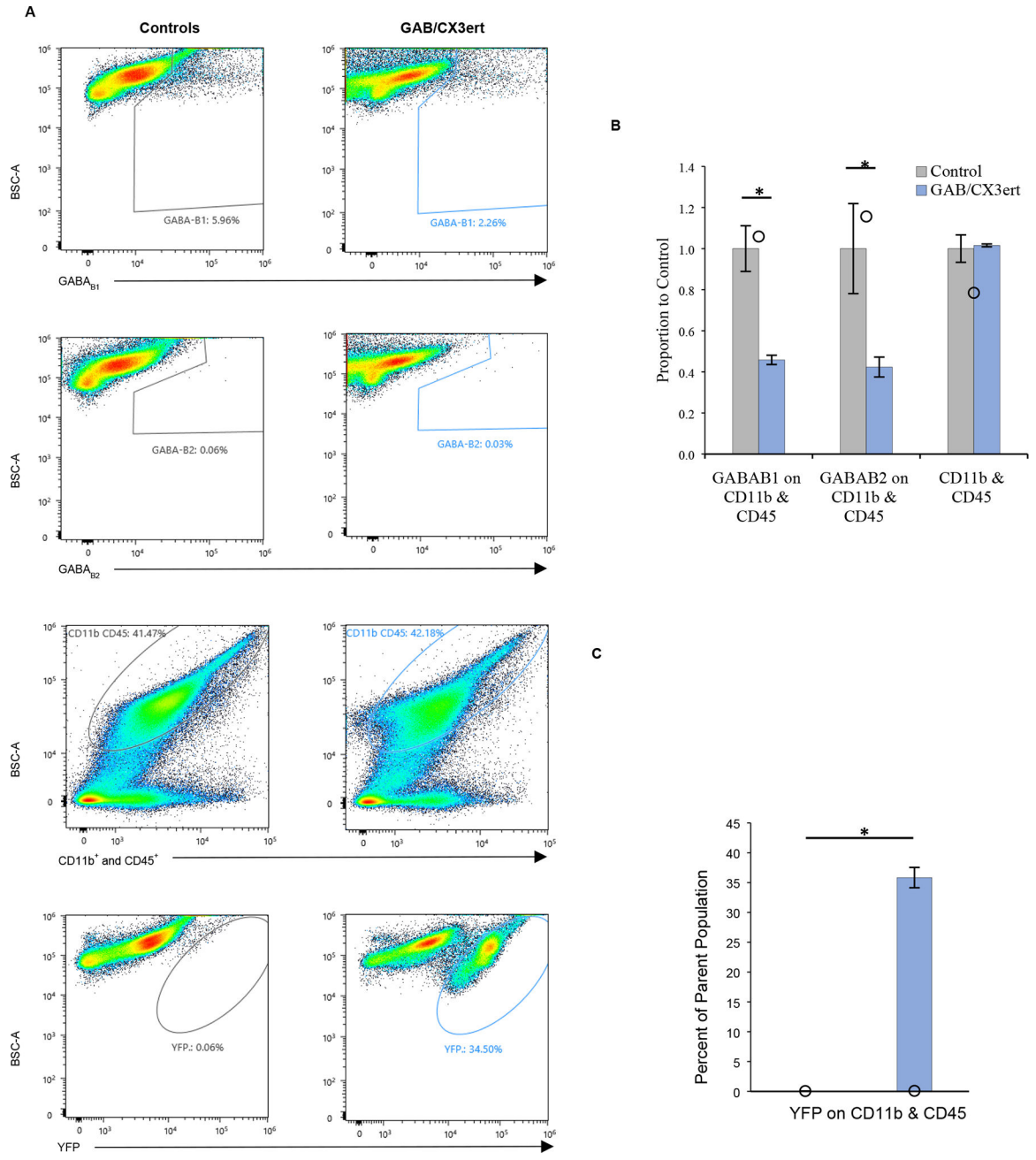

Figure 1. Flow cytometric verification of GABA$_B$1 receptor subunit knockdown and expression of YFP in males.

(A) Representation of gating strategy used for data analysis. (B) Percent of parent population (CD11b$^+$/CD45$^+$) that was positive for GABA$_B$1, GABA$_B$2, and total CD11b$^+$/CD45$^+$ cells. Significant differences in GABA$_B$1 and GABA$_B$2 receptor subunits between controls and GAB/CX3ert mice indicate recombination resulted in knockdown of the GABA$_B$ receptor. (C) YFP is significantly expressed in the GAB/CX3ert mice indicating genetic recombination. Data analysis through IBM SPSS Statistics v24. All data are shown as mean (±SEM); *p<.05.

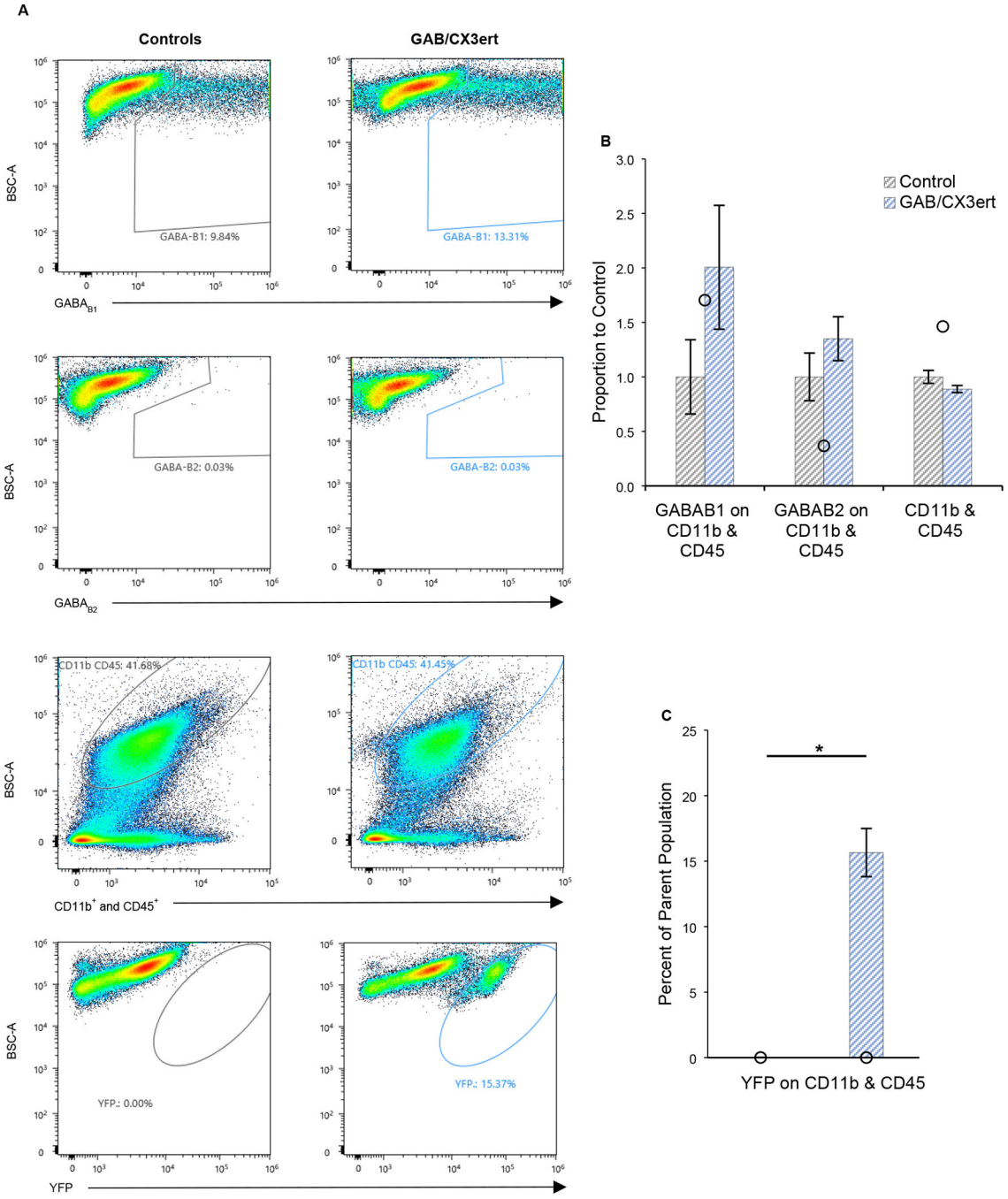

Figure 2. Flow cytometric evaluation of GABA$_B$1 receptor subunit knockdown and expression of YFP in females.

(A) Representation of gating strategy used for data analysis. (B) Percent of parent population (CD11b$^+$/CD45$^+$) that was positive for GABA$_B$1, GABA$_B$2, and total CD11b$^+$/CD45$^+$ cells. No significant differences were observed in GABA$_B$1 and GABA$_B$2 receptor subunits between controls and GAB/CX3ert mice. (C) YFP is significantly expressed in the GAB/CX3ert mice indicating some genetic recombination in samples. Data analysis through IBM SPSS Statistics v24. All data are shown as mean (±SEM); *p<.05.

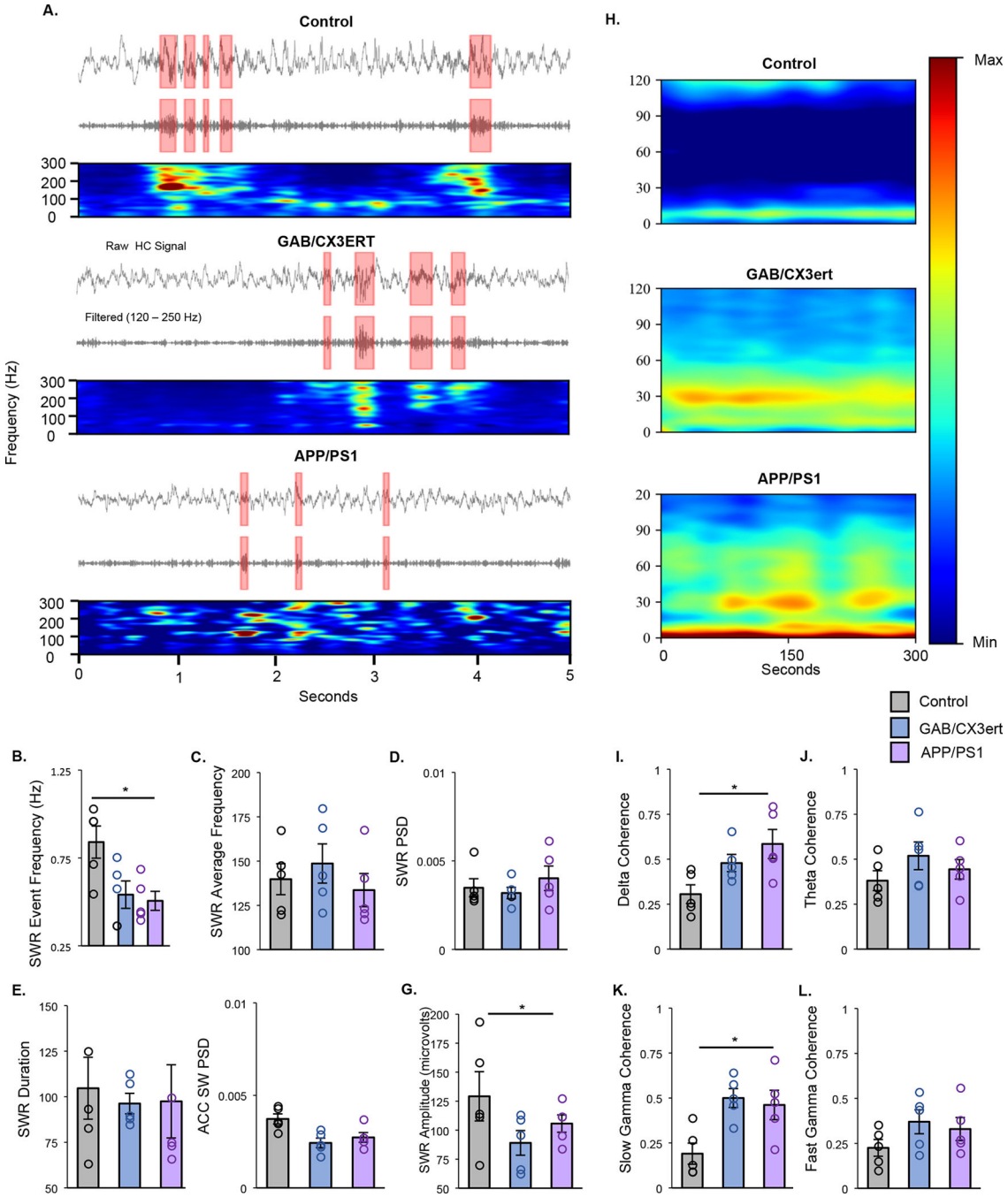

Figure 3. GABA/CX3ert and APP/PS1 mice have fewer sharp-wave ripples and hippocampal-prefrontal hypersynchrony.

(A) Example raw and filtered (150 – 250 (Hz)) traces and spectrograms from C57Bl/6J (top), GABACX3rt (middle), and APP/PS1 (bottom) from raw and filtered hippocampal wires. APP/PS1 and GABA/CX3rt exhibit fewer sharp-wave ripples (SWRs) than C57Bl/6Jmice. (B - G) Comparison of SWR activity of C57Bl/6J, GABACX3rt, and APP/PS1 mice. (B) Frequency of SWR events; (C) Max frequency of hippocampal activity during SWR; (D) max power spectral density in the hippocampus during SWR; (E) duration of SWRs; (F) the maximum amplitude of hippocampal wires during SWR; (G) max power

spectral density in the prefrontal cortex during SWR. Average values are shown for each of the five mice group mean + S.E.M; * $p < 0.05$.

(H - L) Hippocampal - prefrontal Coherence. (H) Average hippocampal - prefrontal coherogram across groups. Note the color bar represents the minimum and maximum coherence values. (I) Delta coherence between the mPFC and HC is higher in APP/PS1 mice than C57Bl/6J and GABA/CX3rt mice. (J) Theta coherence between the mPFC and HC is not significantly different across groups. (K) Slow gamma coherence between the mPFC and HC is significantly higher in APP/PS1 and GABA/CX3rt mice compared to C57Bl/6J. (L) Fast gamma coherence between the mPFC and HC is not significantly different across groups. Average values are shown for each of the five mice group mean + S.E.M; * $p < 0.05$.

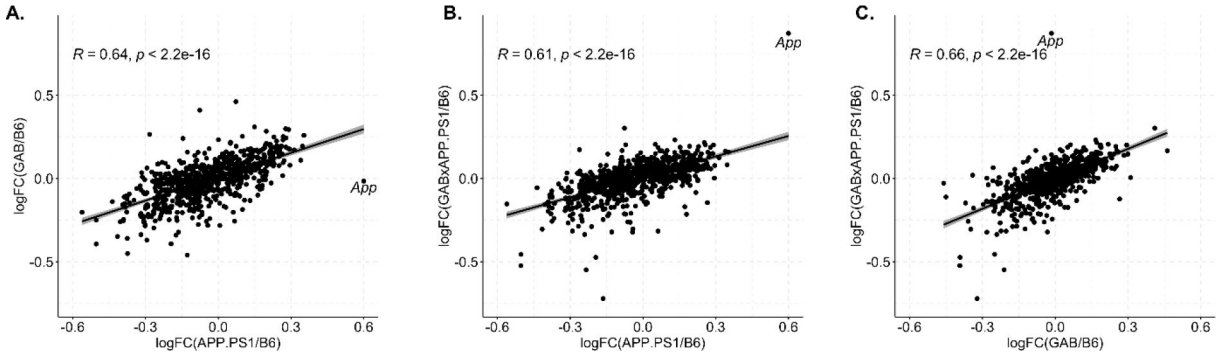

Figure 4: Comparison of gene expression changes of the 770 transcripts on the NanoString panel between pairs of mouse models.

(A) GAB/CX3ert mice showed strong positive correlation (Pearson correlation coefficient = 0.64, $p < 2.2 \times 10^{-16}$) with APP/PS1 mice. (B) GAB/CX3ert x APP/PS1 mice showed strong positive correlation (Pearson correlation coefficient = 0.61, $p < 2.2 \times 10^{-16}$) with APP/PS1 mice.

(C) GAB/CX3ert mice showed strong positive correlation (Pearson correlation coefficient = 0.66, $p < 2.2 \times 10^{-16}$) with GAB/CX3ert x APP/PS1 mice. In all panels the total *App* gene expression is labeled, which reports the sum of the mouse gene and human transgene expression in APP/PS1 carriers, to illustrate the effect of the transgenic construct.

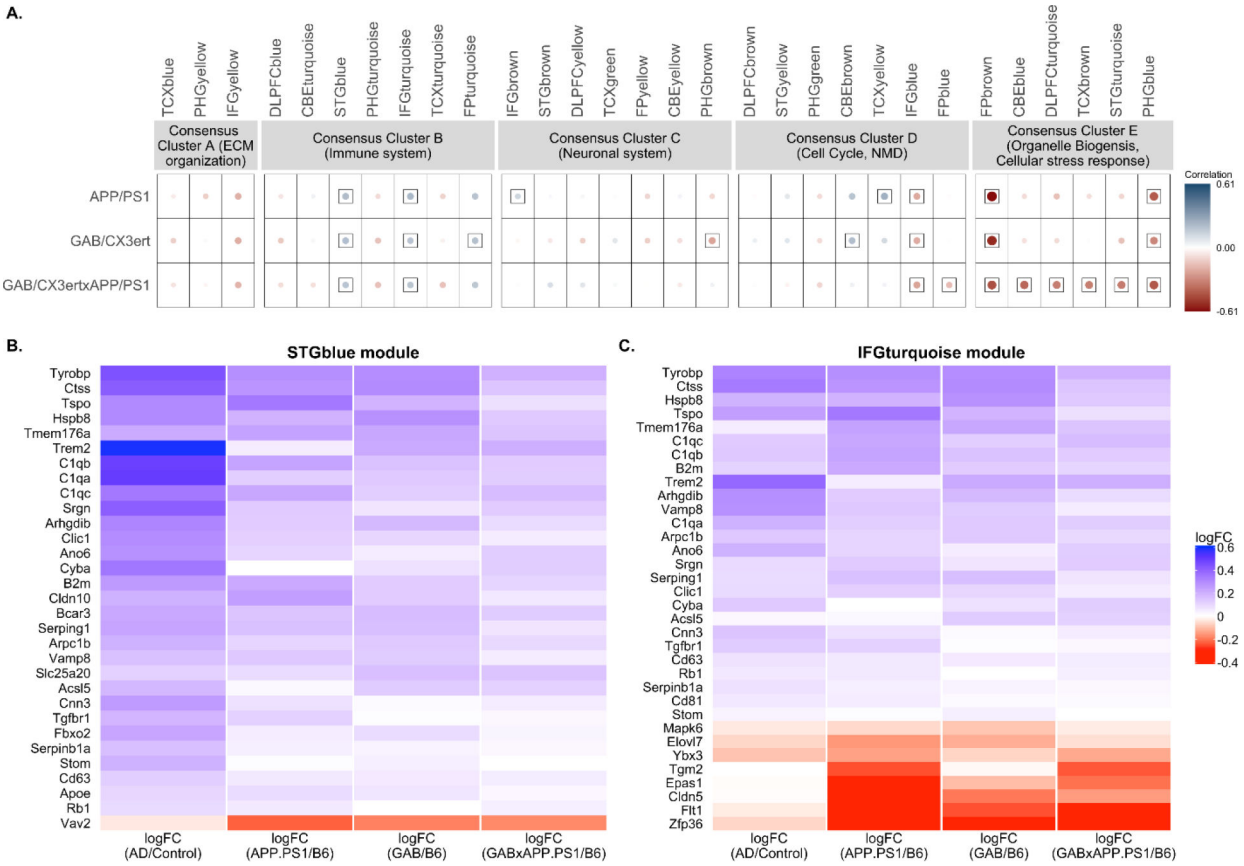

Figure 5: Correlation analysis between mouse models and 30 human co-expression modules using the NanoString Mouse AD panel.

(A) Our mouse models showed a significant positive correlation ($p < 0.05$) with immune related modules STGblue and IFGturquoise in Consensus Cluster B. Circles within a square correspond to significant ($p < 0.05$) positive (blue) and negative (red) Pearson correlation coefficients. Color intensity and size of the circles are proportional to the correlation. (B) Common genes exhibiting directional coherence for gene expression changes between immune related STGblue module and all mouse models. (C) Common genes exhibiting directional coherence for gene expression changes between immune related IFGturquoise module and all mouse models.

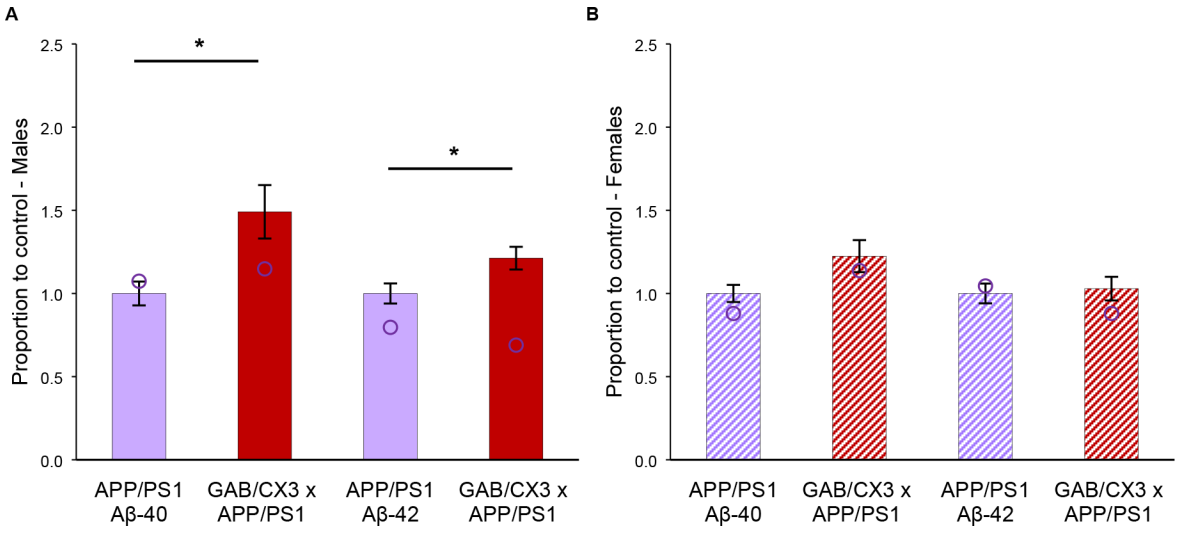

Figure 6. Quantification of Aβ-40 and Aβ-42 in GAB/CX3ert x APP/PS1 mice compared to APP/PS1 mice.

(A) Significant increase in Aβ-40 and Aβ-42 was observed in male GAB/CX3ert mice compared to APP/PS1 mice. (B) No significant differences were observed in female GAB/CX3ert x APP/PS1 mice compared to female APP/PS1 mice. Data analysis through IBM SPSS Statistics v24. All data are shown as mean (±SEM); *p<.05.